

# ALPINE: Unveiling the Planning Capability of Autoregressive Learning in Language Models

Siwei Wang\*                      Yifei Shen\*                      Shi Feng  
 Microsoft Research Asia      Microsoft Research Asia      Harvard University  
 siweiwang@microsoft.com      yifeishen@microsoft.com      shifeng@fas.harvard.edu

Haoran Sun                      Shang-Hua Teng  
 Peking University              University of Southern California  
 sunhaoran0301@stu.pku.edu.cn      shanghua@usc.edu

Wei Chen†  
 Microsoft Research Asia  
 weic@microsoft.com

## Abstract

In this paper, we present the findings of our Project ALPINE which stands for “Autoregressive Learning for Planning In NETWORKS.” Project ALPINE initiates a theoretical investigation into the development of planning capabilities in Transformer-based language models through their autoregressive learning mechanisms, aiming to identify any potential limitations in their planning abilities. We abstract planning as a network path-finding task where the objective is to generate a valid path from a specified source node to a designated target node. In terms of expressiveness, we show that the Transformer is capable of executing path-finding by embedding the adjacency and reachability matrices within its weights. Our theoretical analysis of the gradient-based learning dynamic of the Transformer reveals that the Transformer is capable of learning both the adjacency matrix and a limited form of the reachability matrix. These theoretical insights are then validated through experiments, which demonstrate that the Transformer indeed learns the adjacency matrix and an incomplete reachability matrix, which aligns with the predictions made in our theoretical analysis. Additionally, when applying our methodology to a real-world planning benchmark, called Blocksworld, our observations remain consistent. Our theoretical and empirical analyses further unveil a potential limitation of Transformer in path-finding: it cannot identify reachability relationships through transitivity, and thus would fail when path concatenation is needed to generate a path. In summary, our findings shed new light on how the internal mechanisms of autoregressive learning enable planning in networks. This study may contribute to our understanding of the general planning capabilities in other related domains.

## 1 Introduction

Large language models (LLMs), such as ChatGPT, have impressed everyone with their powerful capabilities in multi-faceted tasks spanning language processing, knowledge extraction, reasoning, planning, coding, tool use, and more. The broad spectrum of intelligent capabilities exhibited by LLMs reflects promising signs of artificial general intelligence (AGI) [BCE<sup>+</sup>23] and catalyzes an AI revolution: Individuals and organizations are now striving to develop more powerful and adaptive AI models towards AGI, while also integrating LLM-based AI models into various aspects of our work and daily lives. However, at the same time, we are still intrigued by the underlying mechanisms that fuel the power of LLMs. While all current LLMs are built upon the Transformer neural network architecture, which employs autoregressive learning to predict the next word in a language sequence, the question remains:

---

\*Equal Contribution

†Contact author

Why does the Transformer-based autoregressive learning architecture produce such exceptional performance across a wide range of intelligent tasks? To put it in plain English: *Why does next word prediction generate intelligence?*

There is no definite answer to this question yet. But researchers are tackling this problem from various angles, aiming to provide explanations to the power of LLMs. In this paper, we focus on the planning capability of LLMs. Planning is a fundamental construct of human intelligence and is involved in almost every aspect of our daily life, e.g., planning a task at work, organizing a trip, seeking a mathematical proof of a theorem, etc. Understanding how LLMs completes a planning task can shed light on the transformation of the seemingly low-level statistical task of next word prediction into a high-level intelligent task like planning. This understanding may serve as a potential pathway to comprehend and explain other intelligent behaviors exhibited by LLMs. There are already a number of studies on the planning capabilities of LLMs. But most of them mainly focus on the empirical evaluation of LLMs. Although these studies may show some evidences that LLMs have planning capabilities to a limited extent, the results are partial and do not explain why LLMs can or cannot successfully accomplish specific planning tasks (see Section 7 for more detailed discussions on the related work).

In light of this context, we initiated Project ALPINE, which stands for Autoregressive Learning for Planning In NETWORKS. Project ALPINE aims to not only empirically evaluate the planning performance of LLMs but also provide theoretical interpretations on how LLMs accomplish such tasks. To provide a solid foundation for our investigation, we must define a specific task that serves as a representative example of a planning task. Given that planning often entails making sequential selections of next steps within a multi-step procedure to achieve a desired goal, it naturally relates to the path-finding task in networks.

A complex task is often represented as a task graph, where nodes correspond to subtasks or intermediate stages, and edges represent the ordering relationships between these subtasks. Task planning involves finding a valid path within the task graph to reach a pre-determined goal. For example, project planning can be viewed as navigating through the multi-stage project planning graph, while a mathematical proof can be seen as a path from the axioms to the final theorem, with lemmas serving as intermediate nodes. Many previous studies on LLM planning capabilities are also related to path finding. For example, a benchmark planning game called Blocksworld [VMSK24] used for evaluating LLMs can be viewed as path finding from the initial blocks' state to the final blocks' state in a state transition graph. Similarly, HuggingGPT [SST+23] for scheduling API calls can be likened to finding a call path in the API call graph.

In Project ALPINE, we investigate the following path-finding task: given an underlying graph, the training data consists of a collection of paths in the graph that specify the source node  $s$ , the target node  $t$  and a path from  $s$  to  $t$ . The objective of the test is to generate a path from  $s'$  to  $t'$ , given new source-target pair  $(s', t')$ .

Note that, for this path-finding task, the generative model must generate a valid path in one shot without relying on trial and error. In this case, the key challenge, when giving the current node on the path, lies in correctly identifying the next node on the path, and this node should be both adjacent to the current node and reachable to the target node (see Algorithm 1). This suggests that in order to accomplish the path-finding task, it is essential to extract the information about the adjacency and reachability of the graph from the training data. Our investigation below demonstrates that the Transformer model is indeed performing this extraction to a certain extent.

More specifically, we investigate how the Transformer-based autoregressive learning architecture achieves the path-finding task by examining the following aspects. First, we show that the Transformer architecture has the expressive power to complete the task by manually constructing a Transformer that encodes the adjacency matrix and reachability matrix of the network as part of its model. Second, we conduct theoretical analysis to further explore the capabilities of the Transformer model. For a simplified Transformer model, when applying gradient descent to minimize the cross-entropy loss on the path training data, our analysis reveals that the model can extract the adjacency matrix and a limited form of the reachability matrix. Specifically, the feed-forward layer encodes the adjacency matrix, while the attention layer captures a partial form of the reachability matrix. This process mimics human intelligence in generating the next node that is both adjacent to the current node and reachable to the target node. However, our theoretical analysis also reveals a limitation of the Transformer model. It cannot learn the full complete reachability relationship. Particularly the reachability derived from

transitivity cannot be learned by the model as the Transformer falls short in capturing these complex reachability patterns.

Third, we conduct extensive experiments that train Transformer models on the path language through autoregressive learning, and test its capability for generating valid paths for new pairs of source and target nodes. Our empirical results provide compelling evidence that the Transformer can excel in achieving high accuracy in the path-finding task. These findings also align with our theoretical analysis as they show that the trained Transformer model generates the next node on the path by focusing its attention on the target node, and effectively learns the adjacency and reachability matrices in its feed-forward layer and attention layer, respectively. Moreover, we observe a significant drop in test accuracy when the source and target can only be connected through concatenation of path segments in the training data. This indicates the requirement for higher-order transitive relationship to establish reachability. This matches our theoretical analysis, showing that the Transformer indeed has limitation in learning transitive reachability relationships. Finally, we demonstrate that the Transformer can successfully learn a task planning benchmark called Blocksworld [VMSK24], a planning task that corresponds directly to the path-finding problem.

In summary, our investigation in Project ALPINE makes the following contributions: (a) We have initiated a theoretical analysis that explains how Transformer achieves a path-planning task through its gradient descent autoregressive learning mechanism; (b) Our empirical evaluation corroborates our theoretical analysis and clearly demonstrates how the Transformer accomplishes path planning by extracting the adjacency and reachability information, while focusing attention on the target node. (c) Both our theoretical and empirical analyses uncover a limitation of the Transformer architecture, highlighting its inability to handle transitive reachability relationship in the path-finding task, which holds significant implications. Our findings represent an initial step toward unraveling the underlying mechanism that empowers the intelligent of LLMs. We believe that this meaningful first step brings us closer to achieving our ultimate objective. We hope that our findings, along with our integrated theoretical and empirical approach, will prove valuable to the community, facilitating collective progress in understanding LLMs and driving improvements future generations of these models.

The rest of the paper is organized as follows. In Section 2, we provide the preliminaries for the study. Section 3 presents an overview of our technical results, including the expressive power of the Transformer model in the path-finding task. In Section 4, we present our theoretical analysis on how a simplified Transformer model solves the path-finding task. Section 5 provides the detailed empirical evaluation results that reinforce our theoretical analysis. Section 6 highlights our findings on the Blocksworld task, which are consistent with our main findings. Following that, in Section 7, we provide an overview of related work and discuss the implications of our results. Finally, we conclude the paper in Section 8.

## 2 Preliminaries

Throughout this paper, we use the following notations for matrices and vectors:  $\mathbf{a}$  and  $\mathbf{A}$  stand for a column vector and a matrix, respectively. Notations  $\mathbf{a}_{(i)}$  and  $\mathbf{A}_{(i,j)}$  denote the  $i^{\text{th}}$  entry of vector  $\mathbf{a}$  and the  $(i,j)^{\text{th}}$  entry in matrix  $\mathbf{A}$ , respectively. We also denote the  $i^{\text{th}}$  row of matrix  $\mathbf{A}$  by  $\mathbf{A}_{(i,:)}$  and the transpose of  $\mathbf{A}$  by  $\mathbf{A}^\top$ .

### 2.1 Auto-regressive Transformer Architecture and Loss Function

In this paper, we adopt the NanoGPT architecture. Let  $N$  denote the sequence length,  $d$  the embedding size,  $H$  the number of heads,  $d_k = d/H$  the embedding size per head, and  $M$  the vocabulary size.

One key component of the architecture is its attention mechanism, which is formulated as

$$\text{Attention}(\mathbf{Q}, \mathbf{K}, \mathbf{V}) = \text{softmax}\left(\frac{\mathbf{Q}\mathbf{K}^\top}{\sqrt{d_k}}\right)\mathbf{V}, \quad (1)$$

where  $\mathbf{Q} \in \mathbb{R}^{N \times d_k}$ ,  $\mathbf{K} \in \mathbb{R}^{N \times d_k}$ ,  $\mathbf{V} \in \mathbb{R}^{N \times d_k}$  are the query, key, and value matrices, respectively. Function **softmax** takes a vector  $\mathbf{a} \in \mathbb{R}^m$  and transforms it into  $\mathbf{b} \in \mathbb{R}^m$  with  $b_i = \frac{e^{a_i}}{\sum_{j=1}^m e^{a_j}}$ . When **softmax** applies to a matrix, it applies to every row of the matrix.

Denoting  $\mathbf{X} \in \mathbb{R}^{N \times d}$  as input, the multi-head attention is computed as

$$\text{MHA}(\mathbf{X}) = \text{Concat}_{i \in [H]}(\text{Attention}(\mathbf{X}\mathbf{W}_i^Q, \mathbf{X}\mathbf{W}_i^K, \mathbf{X}\mathbf{W}_i^V)), \quad (2)$$

where  $\mathbf{W}_i^Q \in \mathbb{R}^{d \times d_k}$ ,  $\mathbf{W}_i^K \in \mathbb{R}^{d \times d_k}$ ,  $\mathbf{W}_i^V \in \mathbb{R}^{d \times d_k}$  are the learnable weight matrices for the query, key, and value matrices of the  $i^{\text{th}}$  head.

The feed-forward layer is a two-layer multi-layer perceptron (MLP) defined as

$$\text{FFN}(\mathbf{X}) = \max(\mathbf{0}, \mathbf{X}\mathbf{W}_1 + \mathbf{1}_{N \times 1}\mathbf{b}_1^\top)\mathbf{W}_2 + \mathbf{1}_{N \times 1}\mathbf{b}_2^\top, \quad (3)$$

where  $\mathbf{W}_1 \in \mathbb{R}^{d \times 4d}$ ,  $\mathbf{W}_2 \in \mathbb{R}^{4d \times d}$ ,  $\mathbf{b}_1 \in \mathbb{R}^{4d}$ , and  $\mathbf{b}_2 \in \mathbb{R}^d$  are the learnable weight matrices of FFN, and  $\mathbf{1}_{N \times x}$  denotes the all-one matrix with dimension  $N \times x$ . Finally, one-layer Transformer is defined as

$$\text{Transformer}(\mathbf{X}) = \text{FFN}(\text{LN}_2(\text{MHA}(\text{LN}_1(\mathbf{X})) + \mathbf{X})) + \text{MHA}(\text{LN}_1(\mathbf{X})) + \mathbf{X}, \quad (4)$$

where  $\text{LN}_1$  and  $\text{LN}_2$  are two layer normalizations. The layer normalization is defined as  $\text{LN}_i(\mathbf{X}) = \frac{\mathbf{X} - \mu}{\sigma + \epsilon} \cdot \gamma_i + \beta_i$ , where the expectation  $\mu \in \mathbb{R}$  and standard deviation  $\sigma \in \mathbb{R}$  are averaged across all terms in  $\mathbf{X}$ ,  $\epsilon = 10^{-5}$ , and  $\gamma_i, \beta_i$  are two learnable scalars.

With these essential components in place, we proceed to introduce the procedures of GPT. The training data consists of a sequence of tokens  $\mathbf{u} = (u_1, \dots, u_N)$ , where  $u_n$  is the token id for the  $n^{\text{th}}$  token. We first represent the tokens by the one-hot embedding matrix  $\mathbf{U} \in \mathbb{R}^{N \times M}$ , where  $\mathbf{U}_{(i, u_i)} = 1$  and 0 elsewhere. Then there is a learnable token embedding matrix  $\mathbf{W}_t \in \mathbb{R}^{M \times d}$  and positional embedding matrix  $\mathbf{W}_p \in \mathbb{R}^{N \times d}$ , and the input  $\mathbf{H}_0 = \mathbf{U}\mathbf{W}_t + \mathbf{W}_p \in \mathbb{R}^{N \times d}$ .

This input  $\mathbf{H}_0$  is fed into an  $L$ -layer Transformer to obtain the predicted next word<sup>1</sup>:

$$\mathbf{H}_l = \text{Transformer}(\mathbf{H}_{l-1}) \in \mathbb{R}^{N \times d}, l = 1, \dots, L. \quad (5)$$

Finally, the output embedding goes through another layer normalization  $\text{LN}_t$ , and then it is multiplied by a learnable output weight matrix  $\mathbf{W}_o \in \mathbb{R}^{d \times M}$  to convert back to probability weights over all possible tokens.

We calculate the output probability vector at position  $n$ , denoted as  $\hat{\mathbf{u}}_{(n+1)}$ , to predict the next token for position  $n + 1$ , which reflects the auto-regressive learning paradigm:

$$\hat{\mathbf{u}}_{(n+1)} = \text{softmax}((\text{LN}_t(\mathbf{H}_L))_{(n,:)}\mathbf{W}_o), 1 \leq n < N. \quad (6)$$

The actual token  $u_{k+1}$  is sampled according to the probability vector  $\hat{\mathbf{u}}_{(n+1)}$  and a temperature parameter. When temperature parameter is set to 1, which is what we use throughout the paper, the sample is directly proportionally to the probability value in  $\hat{\mathbf{u}}_{(n+1)}$ .

The adopted loss function is the cross-entropy loss for the next token prediction given by

$$\ell(\mathbf{U}) = - \sum_{n=1}^{N-1} \sum_{k=1}^M \mathbf{U}_{(n+1,k)} \log \hat{\mathbf{u}}_{(n+1),k}. \quad (7)$$

## 2.2 Path Planning Dataset

The dataset is designed to test GPT’s path planning capability on simple graphs. We consider a directed graph  $\mathcal{G} = (\mathcal{V}, \mathcal{E})$ , where  $\mathcal{V}$  is the set of nodes, and  $\mathcal{E}$  is the set of directed edges, i.e., for any  $u, v \in \mathcal{V}$ ,  $(u, v) \in \mathcal{E}$  means that there is an edge from node  $u$  to node  $v$  in  $\mathcal{G}$ . A pair of source node  $s$  and target node  $t$  is considered as a valid pair if  $\mathcal{G}$  contains least one path from  $s$  to  $t$ . We allocate a portion of valid  $(s, t)$  pairs to the training dataset and assign the remaining pairs to the test dataset.

The samples in the training dataset  $\mathcal{D}$  is sequences of the format “ $s t s a b c t \backslash n$ ”, where  $s$  is the source node,  $t$  is the target node,  $s a b c t$  is a valid path in  $\mathcal{G}$  from  $s$  to  $t$ , and  $\backslash n$  indicates the end of the sequence. In the test dataset, we provide only the source and target nodes in the format “ $s t$ ”. The model is tasked with completing the remaining tokens in the sequence. The completion is deemed correct if the model generates a valid path in graph  $\mathcal{G}$  with the correct syntax.

<sup>1</sup>The learnable weight matrices of different layers are different, and thus the layer index  $l$  should be added as a subscript to these matrices. But our later analysis is only on a one-layer Transformer. Thus we omitted this layer index.

---

**Algorithm 1** A handcrafted path-finding algorithm

---

- 1: **Input:** Adjacency matrix  $\mathbf{A}$ , reachability matrix  $\mathbf{R}$ , source node  $s$ , target node  $t$
  - 2: **Output:** A list contains a path from  $s$  to  $t$
  - 3: Set path node  $P = [s]$  and set current node  $u = s$
  - 4: **while**  $i \neq t$  **do**
  - 5:     Obtain  $S = \{k | \mathbf{A}_{(i,k)} = 1 \text{ and } \mathbf{R}_{(t,k)} = 1\}$
  - 6:     Randomly sample next node  $k$  from  $S$
  - 7:     Add  $k$  to the results  $P = [P; k]$
  - 8:     Set  $i = k$
  - 9: **end while**
- 

### 3 Path-Finding Transformers: Expressive Power and Learning Capacity

In this section, we present an overview of our main results. Firstly, in Theorem 2 below, we establish the mathematical existence of a Transformer model capable of effective path finding in any given network. Next, in Theorem 3—the proof of which will be the main focus of Section 4—we characterize the learning capacity and limitations of path-finding transformer models in a data-driven gradient descent framework. The empirical evaluation that supports these theoretical analyses will be discussed in Section 5.

In our path-finding task, the essential step for completing a path is to predict the next node based on the current information. It is apparent that to predict the subsequent node on the path, only the information related to the current node and the target node is necessary. Algorithm 1 introduces a handcrafted algorithm that utilizes both the adjacency matrix and the reachability matrix of the graph. The true adjacency matrix follows the standard definition in graph theory, i.e.,

$$\mathbf{A}_{(i,k)}^{\text{true}} = \begin{cases} 1, & \text{if } (i, k) \in \mathcal{E}, \\ 0, & \text{otherwise.} \end{cases}$$

The true reachability matrix is defined as:

$$\mathbf{R}_{(t,k)}^{\text{true}} = \begin{cases} 1, & \text{if } k \text{ can reach } t \text{ in } \mathcal{G}, \\ 0, & \text{otherwise.} \end{cases}$$

**Fact 1.** *Assuming that  $t$  is reachable by  $s$ , then Algorithm 1 is guaranteed to output a valid path with input  $\mathbf{A} = \mathbf{A}^{\text{true}}$  and  $\mathbf{R} = \mathbf{R}^{\text{true}}$ .*

To illustrate the expressive capacities of the Transformer model in path finding, we first show that we can manually construct a Transformer model to perform the path planning task by simulating the idealized Algorithm 1. In the manual construction, the task for the model is to find a path from a start node  $s$  to a target node  $t$  with the format “ $s t s u_1 u_2 \dots u_p t$ ”. Consider every time that the Transformer takes “ $s t s u_1 u_2 \dots u_k$ ” as the input and outputs  $u_{k+1}$  for  $k = 0, 1, \dots, p$  (assuming  $s = u_0$  and  $t = u_{p+1}$ ): if  $u_{k+1}$  is an out-neighbor of  $u_k$  and can reach  $t$  in  $\mathcal{G}$ , then we say that the Transformer outputs a correct response.

**Theorem 2** (Expressive Power of the Transformer Model in Path Finding). *Given a graph  $\mathcal{G}$  (with adjacency matrix  $\mathbf{A}^{\text{true}}$  and reachability matrix  $\mathbf{R}^{\text{true}}$ ), for every  $\varepsilon > 0$ , there exists a 1-layer, 1-head, and  $O(|\mathcal{V}|)$ -embedding-size Transformer that makes correct response in every step of the above task with probability at least  $1 - \varepsilon$ .*

*Proof.* For simplicity, we omit all layer normalizations in this construction.

Before presenting the detailed proof, we provide a summary of our construction. In essence, we utilize the attention layer to attend the output *solely* to the target node  $t$ . This approach allows the distribution of next token  $u_{k+1}$  to become a function of both the current node  $u_k$  and the target node  $t$  (as formulated in Section 2). Then, by integrating the adjacency matrix  $\mathbf{A}^{\text{true}}$  into the MLP layer and the reachability matrix  $\mathbf{R}^{\text{true}}$  into the matrix  $\mathbf{W}^V$  in the attention layer, we extract row vectors  $\mathbf{R}_{(t,:)}^{\text{true}}$  and  $\mathbf{A}_{(u_k,:)}^{\text{true}}$  from  $\mathbf{R}^{\text{true}}$  and  $\mathbf{A}^{\text{true}}$ , respectively, corresponding to the target node  $t$  and current node

$u_k$ . Specifically,  $\mathbf{R}_{(t,:)}^{\text{true}}$  and  $\mathbf{A}_{(u_k,:)}^{\text{true}}$  are stored by  $\text{MHA}(\mathbf{H}_0)$  and  $\text{FFN}(\text{MHA}(\mathbf{H}_0) + \mathbf{H}_0)$ , respectively. By selecting proper coefficients, we can ignore the effect of the remaining term  $\mathbf{H}_0$  in  $\text{Transformer}(\mathbf{H}_0)$  and only keep a weighted sum of  $\mathbf{R}_{(t,:)}^{\text{true}}$  and  $\mathbf{A}_{(u_k,:)}^{\text{true}}$ . Following the softmax layer, the non-negligible entries in the final vector correspond to the feasible next nodes. With this encoding, the Transformer serves as a simulator of the idealized Algorithm 1 with input  $\mathbf{A} = \mathbf{A}^{\text{true}}$  and  $\mathbf{R} = \mathbf{R}^{\text{true}}$ .

We now provide the detailed proof. Suppose the input token sequence is “ $s t s u_1 u_2 \dots u_k$ ” with  $k \geq 0$ , where  $s (= u_0)$  and  $t$  are the tokens of the source and target nodes, respectively, and nodes  $s, u_1, \dots, u_k$  form a path that can reach node  $t$  in graph  $\mathcal{G}$ . Our objective is to construct a 1-layer, 1-head Transformer model that consistently generate an out-neighbor  $u_{k+1}$  of  $u_k$ , enabling a path from  $u_k$  to  $t$  in  $\mathcal{G}$ .

Following our notation in Section 2.1, we adopt  $d = |\mathcal{V}| + 2$ ,  $M = |\mathcal{V}| + 1$  and  $N = k + 3$ . In the Transformer, there are  $M = |\mathcal{V}| + 1$  tokens representing the  $|\mathcal{V}|$  nodes and the end-of-line ‘\n’. Hence, the input tokens can be represented by the one-hot embedding matrix  $\mathbf{U} \in \mathbb{R}^{N \times M}$ . We let  $\mathbf{W}_t = (\mathbf{I}_{M \times M} \mid \mathbf{0}_{M \times 1}) \in \mathbb{R}^{M \times d}$  and  $\mathbf{W}_p = (\mathbf{0}_{(k+3) \times (|\mathcal{V}|+1)} \mid c_0 \cdot \mathbf{e}_2) \in \mathbb{R}^{N \times d}$ , here  $\mathbf{e}_2$  represents the second unit column vector of dimension  $k + 3$ ,  $(A \mid B)$  is the notation for matrix concatenation by column, and  $c_0$  is a positive parameter to be decided. According to the definition of the Transformer, we now have a matrix  $\mathbf{H}_0$  such that the first  $|\mathcal{V}| + 1$  columns are the tokens of nodes in the sequence and the last column indicates the positions of the target node  $t$ . More specifically, we have

$$\mathbf{H}_0 = \begin{pmatrix} \mathbf{e}_s^\top & 0 \\ \mathbf{e}_t^\top & c_0 \\ \mathbf{e}_s^\top & 0 \\ \mathbf{e}_{u_1}^\top & 0 \\ \dots & \dots \\ \mathbf{e}_{u_k}^\top & 0 \end{pmatrix} \in \mathbb{R}^{N \times d},$$

here  $\mathbf{e}_u$  represents the one-hot token vector for node  $u$  (with dimension  $M = |\mathcal{V}| + 1$ ).

Then we construct the attention layer of our Transformer. We only have one head and let  $\mathbf{W}^K = (\mathbf{0}_{(|\mathcal{V}|+2) \times (|\mathcal{V}|+1)} \mid \mathbf{1}_{(|\mathcal{V}|+2) \times 1})^\top \in \mathbb{R}^{d \times d}$  and  $\mathbf{W}^Q = \sqrt{d} \cdot \mathbf{I}_{d \times d}$ . Then we can compute  $\mathbf{H}_0 \mathbf{W}^K = (\mathbf{0}_{(|\mathcal{V}|+2) \times 1} \mid c_0 \cdot \mathbf{1}_{(|\mathcal{V}|+2) \times 1} \mid \mathbf{0}_{(|\mathcal{V}|+2) \times (k+1)})^\top$  (i.e. second rows are all  $c_0$ ’s and other rows are all 0’s) and  $\mathbf{H}_0 \mathbf{W}^Q = \sqrt{d} \cdot \mathbf{H}_0$ .

Therefore,

$$\frac{(\mathbf{H}_0 \mathbf{W}^Q)(\mathbf{H}_0 \mathbf{W}^K)^\top}{\sqrt{d}} = \begin{pmatrix} 0 & c_0 & \mathbf{0}_{1 \times (k+1)} \\ 0 & c_0^2 + c_0 & \mathbf{0}_{1 \times (k+1)} \\ \mathbf{0}_{(k+1) \times 1} & c_0 \cdot \mathbf{1}_{(k+1) \times 1} & \mathbf{0}_{(k+1) \times (k+1)} \end{pmatrix} \in \mathbb{R}^{N \times N}.$$

And we can compute the first part of the attention layer as

$$\text{softmax} \left( \frac{(\mathbf{H}_0 \mathbf{W}^Q)(\mathbf{H}_0 \mathbf{W}^K)^\top}{\sqrt{d}} \right) = \begin{pmatrix} \frac{1}{k+2+e^{c_0}} & \frac{e^{c_0}}{k+2+e^{c_0}} & \frac{1}{k+2+e^{c_0}} \cdot \mathbf{1}_{1 \times (k+1)} \\ \frac{1}{k+2+e^{c_0^2+c_0}} & \frac{e^{c_0^2+c_0}}{k+2+e^{c_0^2+c_0}} & \frac{1}{k+2+e^{c_0^2+c_0}} \cdot \mathbf{1}_{1 \times (k+1)} \\ \frac{1}{k+2+e^{c_0}} \cdot \mathbf{1}_{(k+1) \times 1} & \frac{e^{c_0}}{k+2+e^{c_0}} \cdot \mathbf{1}_{(k+1) \times 1} & \frac{1}{k+2+e^{c_0}} \cdot \mathbf{1}_{(k+1) \times (k+1)} \end{pmatrix} \in \mathbb{R}^{N \times N}.$$

By setting  $c_0 \rightarrow +\infty$ , we obtain:

$$\text{softmax} \left( \frac{(\mathbf{H}_0 \mathbf{W}^Q)(\mathbf{H}_0 \mathbf{W}^K)^\top}{\sqrt{d}} \right) \rightarrow \begin{pmatrix} 0 & 1 & \mathbf{0}_{1 \times (k+1)} \\ \dots & \dots & \dots \\ 0 & 1 & \mathbf{0}_{1 \times (k+1)} \end{pmatrix}.$$

Furthermore, we set  $\mathbf{W}^V = \begin{pmatrix} c_1 \cdot \mathbf{R}^{\text{true}} & \mathbf{0}_{|\mathcal{V}| \times 2} \\ \mathbf{0}_{2 \times |\mathcal{V}|} & \mathbf{0}_{2 \times 2} \end{pmatrix}$ , where  $c_1 > 0$  is also a parameter to be decided later. Then after the attention layer, we have a matrix as

$$\lim_{c_0 \rightarrow +\infty} \text{MHA}(\mathbf{H}_0) = c_1 \cdot \begin{pmatrix} \mathbf{R}_{(t,:)}^{\text{true}} & 0 & 0 \\ \dots & \dots & \dots \\ \mathbf{R}_{(t,:)}^{\text{true}} & 0 & 0 \end{pmatrix} \in \mathbb{R}^{N \times d}.$$

Now we construct the feed-forward layer, which is a two-layer MLP.

For the first layer, the weight matrix  $\mathbf{W}_1$  is set to be,

$$\mathbf{W}_1 = \begin{pmatrix} \mathbf{I}_{(|\mathcal{V}|+2) \times (|\mathcal{V}|+2)} & \mathbf{0}_{(|\mathcal{V}|+2) \times 3(|\mathcal{V}|+2)} \end{pmatrix} \in \mathbb{R}^{d \times 4d}.$$

and the bias  $\mathbf{b}_1 = -c_1 \cdot \mathbf{1}_{4d \times 1}$ , which implies that  $\mathbf{1}_{N \times 1} \mathbf{b}_1^\top = -c_1 \cdot \mathbf{1}_{N \times 4d}$ . When  $c_0$  is large enough, the  $(k+3)^{th}$  row of the matrix  $\max(\mathbf{0}, (\text{MHA}(\mathbf{H}_0) + \mathbf{H}_0)\mathbf{W}_1 + \mathbf{1}_{N \times 1} \mathbf{b}_1^\top)$  is  $\max(\mathbf{0}, c_1 \cdot (\mathbf{R}_{(t,:)} | \mathbf{0}_{1 \times (3|\mathcal{V}|+8)}) + (\mathbf{e}_{u_k}^\top | \mathbf{0}_{1 \times (3|\mathcal{V}|+7)}) - c_1 \cdot \mathbf{1}_{1 \times 4(|\mathcal{V}|+2)})$ . Since  $u_k$  can reach  $t$ , in  $c_1 \cdot (\mathbf{R}_{(t,:)} | \mathbf{0}_{1 \times (3|\mathcal{V}|+8)}) + (\mathbf{e}_{u_k}^\top | \mathbf{0}_{1 \times (3|\mathcal{V}|+7)})$ , only the entry for node  $u_k$  is  $c_1 + 1$  while all other entries are 0 or  $c_1$ . Therefore, the  $(k+3)^{th}$  row of the matrix  $\max(\mathbf{0}, (\text{MHA}(\mathbf{H}_0) + \mathbf{H}_0)\mathbf{W}_1 + \mathbf{1}_{N \times 1} \mathbf{b}_1^\top)$  can be arbitrarily close to  $(\mathbf{e}_{u_k}^\top | \mathbf{0}_{1 \times (3|\mathcal{V}|+7)})$ . Here  $\mathbf{e}_u$  represents the one-hot token vector for node  $u$  (with dimension  $M = |\mathcal{V}| + 1$ ).

For the second layer, we set

$$\mathbf{W}_2 = \begin{pmatrix} c_2 \cdot \mathbf{A} & \mathbf{0}_{|\mathcal{V}| \times 2} \\ \mathbf{0}_{(3|\mathcal{V}|+8) \times |\mathcal{V}|} & \mathbf{0}_{(3|\mathcal{V}|+8) \times 2} \end{pmatrix} \in \mathbb{R}^{4d \times d},$$

where  $c_2$  are positive parameters to be decided, and  $\mathbf{b}_2 = \mathbf{0}$ . By this way, we have

$$\lim_{c_0 \rightarrow \infty} (\text{FFN}(\text{MHA}(\mathbf{H}_0) + \mathbf{H}_0))_{(k+3,:)} \rightarrow (c_2 \cdot \mathbf{A}_{(u_k,:)} | \mathbf{0}_{1 \times 2}) \in \mathbb{R}^{|\mathcal{V}|+2}.$$

Therefore,

$$\lim_{c_0 \rightarrow \infty} (\mathbf{H}_1)_{(k+3,:)} \rightarrow (c_1 \cdot \mathbf{R}_{(t,:)} + c_2 \cdot \mathbf{A}_{(u_k,:)} | \mathbf{0}_{1 \times 2}) + (\mathbf{e}_{u_k} | 0) \in \mathbb{R}^{|\mathcal{V}|+2},$$

where  $\mathbf{e}_u$  represents the one-hot token vector for node  $u$  (with dimension  $M = |\mathcal{V}| + 1$ ).

Then we fix  $c_1 = c_2$  and let them be large enough. In this case, the dominant entries in  $(\mathbf{H}_1)_{(k+3,:)}$  represent the nodes that are both the out-neighbor of  $u_j$  and reachable to  $t$ , since those entries will have the value of  $2c_1$  while others entries are at most  $c_1 + 1$ . This means that  $(\mathbf{H}_1)_{(k+3,:)}$  can correctly indicate the next node  $u_{k+1}$ . Specifically, let  $\mathbf{W}_o = (\mathbf{I}_{(|\mathcal{V}|+1) \times (|\mathcal{V}|+1)} | \mathbf{0}_{(|\mathcal{V}|+1) \times 1})^\top \in \mathbb{R}^{d \times M}$ . Then the final output approaches the following vector

$$\begin{aligned} \lim_{c_0, c_1 = c_2 \rightarrow \infty} \hat{u}_{k+1} &= \lim_{c_0, c_1 = c_2 \rightarrow \infty} \text{softmax}((\mathbf{H}_1)_{(k+3,:)} \mathbf{W}_o) \\ &= \frac{1}{C} \cdot (\mathbb{I}[\mathbf{A}_{(u_k,1)} = 1 \wedge \mathbf{R}_{(t,1)} = 1], \dots, \mathbb{I}[\mathbf{A}_{(u_k,|\mathcal{V}|)} = 1 \wedge \mathbf{R}_{(t,|\mathcal{V}|)} = 1], 0), \end{aligned}$$

where  $C$  is the number of nodes that are both the out-neighbor of  $u_k$  and reachable to  $t$ . Thus, this encoding guarantees that this is exactly the correct output of the next node. Hence, for any  $\varepsilon > 0$ , we can always find a 1-layer, 1-head, and  $(|\mathcal{V}| + 2)$ -embedding-size Transformer that provides the correct response with probability at least  $1 - \varepsilon$  by selecting large enough parameters  $c_0, c_1, c_2$ .

Finally, there are two different rules (other than output a correct next node): i) when the input sequence is only “ $s t$ ”, the prediction of the next token should be the source node  $s$ ; ii) when the input sequence is only “ $s t s a b c t$ ”, the prediction of the next token should be  $\backslash n$ . Case i) can be constructed using the Transformer architecture utilizing the position information and attention to the first position; and case ii) can be constructed by using the Transformer architecture utilizing the position information and attention to the second position. To maintain focus on the main construction corresponding to Algorithm 1, we omit the detailed construction for these two boundary cases.  $\square$

Having established the mathematical existence of a Transformer model capable of accomplishing path finding in a given network, as demonstrated in Theorem 2, we now shift our focus to the following fundamental question

*Can the Transformer architecture, trained on sufficient path data with an auto-regressive loss as in Equation (7) and using the gradient descent (GD) method, learn the adjacency and reachability matrices and carry out path finding similar to the idealized Algorithm 1?*

Through a combination of theoretical analysis and empirical evaluation presented in the following section, our primary investigation aims to address the aforementioned question.

First, it is important to note that the Transformer may not be capable to learn the exact true adjacency and reachability matrices of the underlying graph. Instead, it can only learn the relevant

information that is directly encoded in the observed training data  $\mathcal{D}$ . Therefore, we define the *observed* adjacency and reachability matrices based on the training data  $\mathcal{D}$  as follows.

$$\mathbf{A}_{(i,k)}^{\text{obs}}(\mathcal{D}) = \begin{cases} 1, & \text{if } \exists \mathbf{u} \in \mathcal{D}, n \in [3, N-1] \text{ s.t. } u_n = i, u_{n+1} = k \\ 0, & \text{otherwise} \end{cases}$$

$$\mathbf{R}_{(t,k)}^{\text{obs}}(\mathcal{D}) = \begin{cases} 1, & \text{if } \exists \mathbf{u} \in \mathcal{D}, n \in [4, N] \text{ s.t. } u_2 = t, u_n = k \\ 0, & \text{otherwise.} \end{cases}$$

Naturally, the observed adjacency matrix  $\mathbf{A}^{\text{obs}}(\mathcal{D})$  only records the edges  $(i, k)$  that appears in some path within the training data  $\mathcal{D}$ . On the other hand, the observed reachability matrix  $\mathbf{R}^{\text{obs}}(\mathcal{D})$  exhibits more nuanced distinctions from the true reachability matrix. It only records that  $t$  is reachable from node  $k$ , if the training data  $\mathcal{D}$  contains a path (sequence) whose destination is  $t$  and  $k$  appears as a non-source node on the path. We call such pairs  $(t, k)$  *observed reachable pairs*. Therefore, the observed reachability matrix would miss the following types of reachable pairs  $(t, k)$  in  $\mathcal{G}$  (referred as non-observed reachable pairs): (i) there is no path in  $\mathcal{D}$  that contains a sub-path from  $k$  to  $t$ , even if a path from  $k$  to  $t$  can be obtained by concatenating several sub-paths appeared in  $\mathcal{D}$ ; (ii) there are some paths in  $\mathcal{D}$  that contains a sub-path from  $k$  to  $t$ , however,  $t$  is not the target node in these paths; (iii) there are some paths in  $\mathcal{D}$  that contains a sub-path from  $k$  to  $t$  and  $t$  is the target node in these paths, however,  $k$  is always the source node of these paths.

In Section 4, we show that in a simplified Transformer model, the learning is limited to the observed adjacency and reachability matrices, rather than the true underlying matrices. The following presents an informal version of the result:

**Theorem 3** (Learning Capacity and Limitation of Path-Finding Transformer: An Informal version). *By using auto-regressive loss and training with gradient descent, a simplified Transformer architecture with 1-layer, 1-head, and  $O(|\mathcal{V}|)$ -embedding-size simulates Algorithm 1 with  $\mathbf{R} = \mathbf{R}^{\text{obs}}(\mathcal{D})$  and  $\mathbf{A} = \mathbf{A}^{\text{obs}}(\mathcal{D})$ .*

The formal analytical result is presented as Theorem 4, which gives captures the direction of changes of the parameters in the learnable matrices of the simplified Transformer when following the gradient descent calculation. We then discuss that how this result indicates that the simplified Transformer effectively learns the observed adjacency matrix and the observed reachability matrix, and its inference procedure indeed align with the workings of Algorithm 1. Specifically, in the simplified Transformer, the observed adjacency matrix is encoded within the weights of the feed-forward network (FFN) as illustrated in Figure 1, while the observed reachability matrix is encoded in the value matrix, as depicted in Figure 2.

Next, in Section 5, we present the results of our empirical evaluation which is based on extensive experiments. We report the accuracy achieved by the Transformer models with various hyperparameters (Figure 3). Furthermore, we provide visualizations that demonstrate the Transformer’s ability to learn attention (Figure 4) as well as the information about adjacency and reachability matrices (Figures 5 and 6). Notably, our findings reveal that even a large Transformer model fails to learn the reachability matrix beyond  $\mathbf{R}^{\text{obs}}(\mathcal{D})$ , resulting poor path-finding accuracy for those unobserved reachable pairs (Figure 6). To further validate our approach, we conduct experiments on a realistic planning dataset called Blocksworlds. The accuracy, attention, adjacency matrix and reachability matrix are shown in Figure 7 and Figure 8. Importantly, our empirical results align closely with our theoretical findings discussed in Section 4.

## 4 Gradient-based Analysis for Path Finding

Let  $\mathcal{D}$  be the path dataset as described in Section 2.2. In this section, we show analytically that even with only one layer and one head, the Transformer architecture could learn both the adjacency matrix and the reachability matrix from the dataset  $\mathcal{D}$  and then predict the next node on a path, similar to what is done in Algorithm 1. Let  $N_{i,j,k}$  be the number of times in  $\mathcal{D}$  that i) the current node is  $i$ ; ii) the destination node is  $j$  and iii) the next node is  $k$ , and let  $N_{i,j} = \sum_k N_{i,j,k}$ .



To simplify the analysis, we consider the following simplified *one* layer and *one* head Transformer structure without any layer normalizations. The embedding size is the same as the vocabulary size ( $d = M$ ), and we only consider the cross-entropy loss of predicting the next node, i.e., only when  $n \geq 3$  (hence it is not repeating the source node) and the token  $u_n$  is not the target node (hence it is not predicting “\n”).

- The attention weight is only on the target node (the second token), i.e., we manually set every row in  $\mathbf{softmax}\left(\frac{\mathbf{QK}^\top}{\sqrt{d_k}}\right)$  (in Eq. (1)) to be a one-hot vector with the second coordinate being 1. Moreover, we set the positional embedding matrix  $\mathbf{W}_p = \mathbf{0}$ , since it is usually used to adjust the attention weights<sup>2</sup>.
- We remove all the non-linear layers (e.g., the layer normalizations), and use  $\text{FFN}(\mathbf{X}) = \mathbf{X}\mathbf{W}^M$  instead of Eq. (3), and use  $\text{Transformer}(\mathbf{X}) = \text{FFN}(\mathbf{X}) + \text{MHA}(\mathbf{X})$  instead of Eq. (4).
- The token embedding matrix  $\mathbf{W}_t$  and the output weight matrix  $\mathbf{W}_o$  are set to be identity, i.e.,  $\mathbf{W}_t = \mathbf{W}_o = \mathbf{I}$ .

Since there is only one layer and one head, for simplicity, we use  $\mathbf{W}^V$  to represent the weight of the value matrix in the attention layer. Under the above Transformer structure,

$$(\mathbf{H}_L)_{(n,:)}\mathbf{W}_o = (\mathbf{U}\mathbf{W}_t\mathbf{W}^M + \alpha\mathbf{U}\mathbf{W}_t\mathbf{W}^V)_{(n,:)}\mathbf{W}_o = (\mathbf{U}\mathbf{W}^M + \alpha\mathbf{U}\mathbf{W}^V)_{(n,:)} = \mathbf{W}_{(u_n,:)}^M + \mathbf{W}_{(u_2,:)}^V, \quad (8)$$

where  $\alpha$  is the manually set attention weight matrix (every row is a one-hot vector with the second coordinate being 1). Therefore, the weight vector when predicting the  $(n + 1)^{\text{th}}$  token is  $\mathbf{softmax}(\mathbf{W}_{(u_n,:)}^M + \mathbf{W}_{(u_2,:)}^V)$ , and the prediction probability is

$$\hat{u}_{n+1,k} = \frac{\exp(\mathbf{W}_{(u_n,k)}^M + \mathbf{W}_{(u_2,k)}^V)}{\sum_{\ell} \exp(\mathbf{W}_{(u_n,\ell)}^M + \mathbf{W}_{(u_2,\ell)}^V)}. \quad (9)$$

We prove the following theorem.

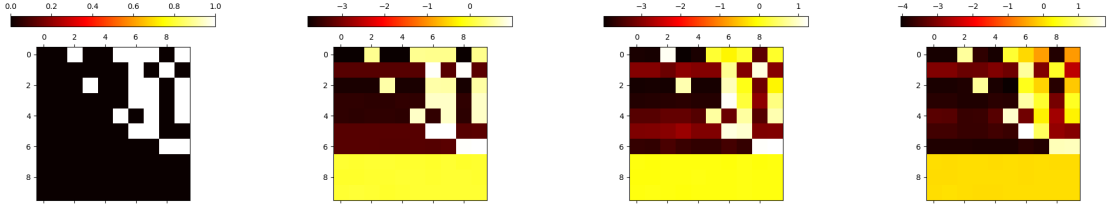
**Theorem 4.** *Under the cross-entropy loss  $\ell(\mathcal{D})$ , for all possible  $(i, k)$  pairs, i) if  $\sum_j N_{i,j} = 0$ , then  $\frac{\partial \ell(\mathcal{D})}{\partial \mathbf{W}_{(i,k)}^M}$  is always 0; ii) if  $\sum_j N_{i,j} > 0$  but  $\sum_j N_{i,j,k} = 0$ , then  $\frac{\partial \ell(\mathcal{D})}{\partial \mathbf{W}_{(i,k)}^M}$  is always positive; iii) if  $\sum_j N_{i,j,k} > 0$ , then  $\frac{\partial \ell(\mathcal{D})}{\partial \mathbf{W}_{(i,k)}^M}$  is negative when  $\mathbf{W}_{(i,k)}^M$  converges to  $-\infty$ . Similarly, for all possible  $(j, k)$  pairs, i) if  $\sum_i N_{i,j} = 0$ , then  $\frac{\partial \ell(\mathcal{D})}{\partial \mathbf{W}_{(j,k)}^V}$  is always 0; ii) if  $\sum_i N_{i,j} > 0$  but  $\sum_i N_{i,j,k} = 0$ , then  $\frac{\partial \ell(\mathcal{D})}{\partial \mathbf{W}_{(j,k)}^V}$  is always positive; iii) if  $\sum_i N_{i,j,k} > 0$ , then  $\frac{\partial \ell(\mathcal{D})}{\partial \mathbf{W}_{(j,k)}^V}$  is negative when  $\mathbf{W}_{(j,k)}^V$  converges to  $-\infty$ .*

*Proof.* We only prove the first part of this theorem, since the proof of the second part is almost the identical.

By the definition of the cross-entropy loss in Eq.(7), and the prediction weight vector in Eq.(9) for

---

<sup>2</sup>This corresponds to the perfect attention case, and is a mild assumption since =====



(a) True adjacency matrix  $\mathbf{A}^{\text{true}} = \mathbf{A}^{\text{obs}}(\mathcal{D}_1) = \mathbf{A}^{\text{obs}}(\mathcal{D}_2) = \mathbf{A}^{\text{obs}}(\mathcal{D}_3)$  (b) Matrix  $\mathbf{W}^M$  under  $\mathcal{D}_1$  (c) Matrix  $\mathbf{W}^M$  under  $\mathcal{D}_2$  (d) Matrix  $\mathbf{W}^M$  under  $\mathcal{D}_3$

Figure 1: Empirical verification regarding the learning of the adjacency matrix.

our simplified model, the total cross-entropy loss of the model (with matrices  $\mathbf{W}^M, \mathbf{W}^V$ ) is

$$\begin{aligned}
\ell(\mathcal{D}) &= - \sum_{U \in \mathcal{D}} \sum_{n \geq 3} \sum_k U_{(n+1,k)} \log \hat{u}_{(n+1),k} \\
&= - \sum_{U \in \mathcal{D}} \sum_{n \geq 3} \sum_k U_{(n+1,k)} \log \frac{\exp(\mathbf{W}_{(u_n,k)}^M + \mathbf{W}_{(u_2,k)}^V)}{\sum_{\ell} \exp(\mathbf{W}_{(u_n,\ell)}^M + \mathbf{W}_{(u_2,\ell)}^V)} \\
&= - \sum_{U \in \mathcal{D}} \sum_{n \geq 3} \sum_k U_{(n+1,k)} \sum_{i,j} \mathbb{I}[u_n = i, u_2 = j] \log \frac{\exp(\mathbf{W}_{(i,k)}^M + \mathbf{W}_{(j,k)}^V)}{\sum_{\ell} \exp(\mathbf{W}_{(i,\ell)}^M + \mathbf{W}_{(j,\ell)}^V)} \\
&= - \sum_{i,j,k} N_{i,j,k} \log \frac{\exp(\mathbf{W}_{(i,k)}^M + \mathbf{W}_{(j,k)}^V)}{\sum_{\ell} \exp(\mathbf{W}_{(i,\ell)}^M + \mathbf{W}_{(j,\ell)}^V)} \\
&= - \sum_{i,j,k} N_{i,j,k} (\mathbf{W}_{(i,k)}^M + \mathbf{W}_{(j,k)}^V) + \sum_{i,j,k} N_{i,j,k} \log \left( \sum_{\ell} \exp(\mathbf{W}_{(i,\ell)}^M + \mathbf{W}_{(j,\ell)}^V) \right) \\
&= - \sum_{i,j,k} N_{i,j,k} (\mathbf{W}_{(i,k)}^M + \mathbf{W}_{(j,k)}^V) + \sum_{i,j} N_{i,j} \log \left( \sum_{\ell} \exp(\mathbf{W}_{(i,\ell)}^M + \mathbf{W}_{(j,\ell)}^V) \right).
\end{aligned}$$

Then we have that

$$\frac{\partial \ell(\mathcal{D})}{\partial \mathbf{W}_{(i,k)}^M} = - \sum_j N_{i,j,k} + \frac{\exp(\mathbf{W}_{(i,k)}^M + \mathbf{W}_{(j,k)}^V)}{\sum_{\ell} \exp(\mathbf{W}_{(i,\ell)}^M + \mathbf{W}_{(j,\ell)}^V)} \cdot \sum_j N_{i,j}. \quad (10)$$

In case i),  $\sum_j N_{i,j} = 0$  implies that  $\sum_j N_{i,j,k} = 0$ . Hence  $\frac{\partial \ell(\mathcal{D})}{\partial \mathbf{W}_{(i,k)}^M}$  is always zero.

In case ii),  $\sum_j N_{i,j} > 0$  implies that the second term in Eq. (10) is positive, while  $\sum_j N_{i,j,k} = 0$  implies that the first term in Eq. (10) is 0. Hence  $\frac{\partial \ell(\mathcal{D})}{\partial \mathbf{W}_{(i,k)}^M}$  is always positive.

In case iii), when  $\sum_j N_{i,j} > 0$  and  $\mathbf{W}_{(i,k)}^M$  converges to  $-\infty$ , then the second term in Eq. (10) converges to zero, and it is smaller than  $\sum_j N_{i,j,k} > 0$ . Hence,  $\frac{\partial \ell(\mathcal{D})}{\partial \mathbf{W}_{(i,k)}^M}$  is negative when  $\mathbf{W}_{(i,k)}^M$  converges to  $-\infty$ .  $\square$

The theorem directly leads to a theoretical explanation on how the model learns the adjacency and reachability matrices, as explained below.

**Learning the adjacency matrix.** Let  $\mathcal{E}(\mathcal{D})$  denote the set of edges appearing in the training dataset  $\mathcal{D}$ , which corresponds to the observed adjacency matrix  $\mathbf{A}^{\text{obs}}(\mathcal{D})$ . For any  $(i, k) \in \mathcal{E}(\mathcal{D})$ ,  $\sum_j N_{i,j,k} > 0$ , and for any  $(i', k') \notin \mathcal{E}(\mathcal{D})$ ,  $\sum_j N_{i',j,k'} = 0$ . Then from the above theorem, under the gradient descent learning paradigm,  $\mathbf{W}_{(i',k')}^M$  will keep decreasing (since its gradient is always positive), while  $\mathbf{W}_{(i,k)}^M$  will not (since its gradient becomes negative when its value is sufficiently negative). This tends to make

$\mathbf{W}_{(i,k)}^M$  higher than  $\mathbf{W}_{(i',k')}^M$  after training. Note that these terms are weights when predicting the next node: a higher  $\mathbf{W}_{(i,k)}^M$  means that “the edge  $(i, k)$  exists”, and a lower  $\mathbf{W}_{(i',k')}^M$  means that “the edge  $(i', k')$  does not exist”. By this way, the Transformer model *learns the information about the observed adjacency matrix* with weight matrix  $\mathbf{W}^M$ .

To facilitate comprehension, we conducted a simple experiment, and present the results in Figure 1 (the structure of the Transformer aligns with the description provided in this section). In this experiment, we generate a 10-node graph, and use 3 different training datasets  $\mathcal{D}_1, \mathcal{D}_2, \mathcal{D}_3$  based on this graph:  $\mathcal{D}_1$  contains all the paths with length 1;  $\mathcal{D}_2$  contains all the paths with length 1 and 20% of the paths with length higher than 1; and  $\mathcal{D}_3$  contains all the possible paths. Figure 1(a) is the true adjacency matrix of the graph, which is also the observed adjacency matrix for the three datasets. Figure 1(b) is the  $\mathbf{W}^M$  matrix with the training dataset  $\mathcal{D}_1$ , Figure 1(c) is the  $\mathbf{W}^M$  matrix with the training dataset  $\mathcal{D}_2$ , and Figure 1(d) is the  $\mathbf{W}^M$  matrix with the training dataset  $\mathcal{D}_3$ <sup>3</sup>. Upon observation, it becomes evident that these  $\mathbf{W}^M$  matrices all successfully capture the structural information from the adjacency matrix. Specifically, in the  $i^{\text{th}}$  row of each of these weight matrices, the  $k^{\text{th}}$  term corresponding to edge  $(i, k) \in \mathcal{E}$  is much higher than the  $k^{\text{th}}$  term corresponding to non-edge  $(i, k) \notin \mathcal{E}$ .

**Learning the reachability matrix.** Similar to the process of learning the adjacency matrix, under the gradient descent learning paradigm,  $\mathbf{W}_{(j',k')}^V$  will keep decreasing when  $(j', k')$  is not an observed reachable pairs in the training dataset  $\mathcal{D}$ . In other words, there is no path in  $\mathcal{D}$  in which  $j'$  is the target and  $k'$  is a non-source node on the path. On the other hand, when  $(j, k)$  is indeed an observed reachable pair,  $\mathbf{W}_{(j,k)}^V$  does not keep decreasing. This tends to make  $\mathbf{W}_{(j,k)}^V$  higher than  $\mathbf{W}_{(j',k')}^V$  after the training. By this way, the Transformer model *captures the structural information of observed reachability matrix* with weight matrix  $\mathbf{W}^V$ . However, our analysis indicates that the model may not learn non-observed reachability relationship even if all the edges are present in the training data. These non-observed reachable pairs  $(j, k)$  encompass several cases, which are summarized in Section 3.

Figure 2 shows the correlation between  $\mathbf{W}^V$  and the observed reachabilities under different dataset  $\mathcal{D}$ 's in the above simple experiment. Figure 2(a) is the real reachability matrix of the graph; Figure 2(b) is the observed reachability matrix in dataset  $\mathcal{D}_1$ , and Figure 2(c) is the  $\mathbf{W}^V$  matrix under  $\mathcal{D}_1$ ; Figure 2(d) is the observed reachability matrix in dataset  $\mathcal{D}_2$ , and Figure 2(e) is the  $\mathbf{W}^V$  matrix under  $\mathcal{D}_2$ ; and similarly, Figure 2(f) is the observed reachability matrix in dataset  $\mathcal{D}_3$ , and Figure 2(g) is the  $\mathbf{W}^V$  matrix under  $\mathcal{D}_3$ . These illustrations shows all the weight matrices  $\mathbf{W}^V$  can satisfactorily learn the structural information of the observed reachabilities present in the training datasets.

However, the Transformer models cannot deduce non-observed reachabilities. In particular, we demonstrate that all three types of non-observed reachable pairs as summarized in Section 3 appear in this example: (i) there is no paths that contain the sub-paths from node 5 to nodes 8 and 9 in  $\mathcal{D}_1$  and  $\mathcal{D}_2$ , hence the reachable pairs  $(8, 5)$  and  $(9, 5)$  are not learned in these two cases (the corresponding entries  $(8, 5)$  and  $(9, 5)$  in Figure 2(c) and Figure 2(d) are dark), even though that from these two datasets the model can learn that 5 reaches 6, 6 reaches 7, 7 reaches 8, and 8 reaches 9 separately; (ii) there is a path “0 9 0 2 3 9” in  $\mathcal{D}_2$ , but the reachable pair  $(3, 2)$  is not learned (the corresponding entry  $(3, 2)$  in Figure 2(d) is dark red); and (iii) none of these matrices learn the reachable pairs of  $(j, k)$  with  $k = 0, 1, 4$ , since nodes 0, 1, 4 never appear as a non-source node in a path.

**Predicting the next node on a path.** From Eq.(9), we know that the probability vector for predicting the next node is given as  $\mathbf{softmax}(\mathbf{W}_{(u_n,:)}^M + \mathbf{W}_{(u_2,:)}^V)$ , where  $u_n$  represents the current node, and  $u_2$  represents the target node. This provides an intuitive explanation for why  $\mathbf{W}^M$  learns the observed adjacency matrix, while  $\mathbf{W}^V$  learns the observed reachability matrix. The mechanism utilizes  $\mathbf{W}^M$  on the current node  $u_n$  to provide information about the next node it connects to, whereas  $\mathbf{W}^V$  is used on the target node to provide information on which nodes can reach the target node. The softmax operation  $\mathbf{softmax}(\mathbf{W}_{(u_n,:)}^M + \mathbf{W}_{(u_2,:)}^V)$  resembles the procedure in Algorithm 1: it predicts the next node  $k$  such that both  $\mathbf{W}_{(u_n,k)}^M$  is high (corresponding to  $\mathbf{A}(u_n, k) = 1$ ) and  $\mathbf{W}_{(u_2,k)}^V$  is high (corresponding to  $\mathbf{R}(u_2, k) = 1$ ).

<sup>3</sup>Matrix  $\mathbf{W}^M$  also contains rows and columns corresponding to non-node tokens such as ‘\n’, and we remove these rows and columns in the comparison. Later when we compare empirical matrices  $\mathbf{W}^V$  and  $\mathbf{W}_t \mathbf{W}_1 \mathbf{W}_2 \mathbf{W}_o$  against theoretical ones, we treat them in the same way.

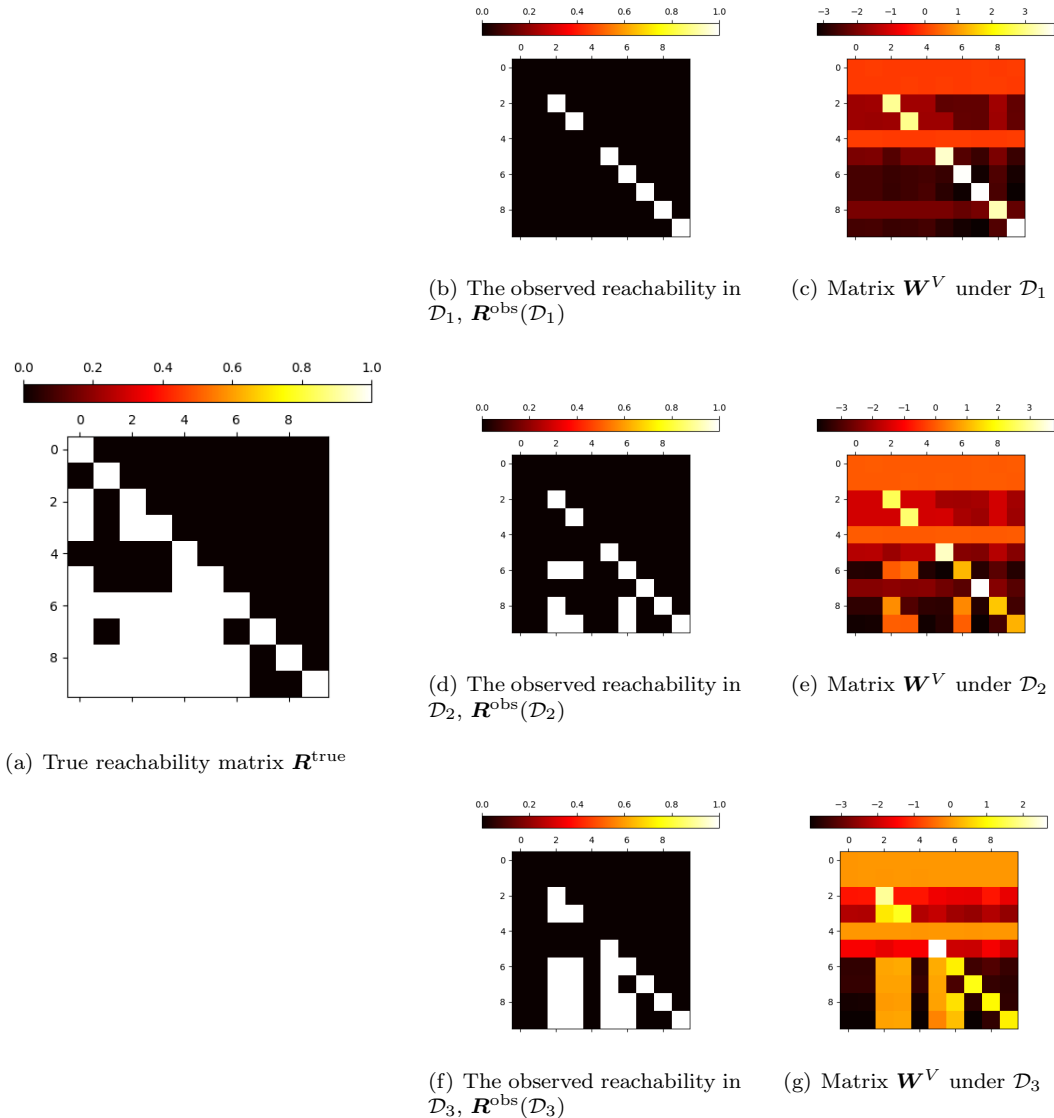


Figure 2: Empirical verification regarding the learning of the observed reachability matrix.

In summary, our theoretical analysis demonstrates that a simplified one-layer, one-head autoregressive Transformer (with perfect attention) can effectively learn crucial adjacency and reachability information from the training data through gradient descent training. Moreover, it can utilize this learned information to predict the next node akin to the decision-making process of a human algorithm designer in similar scenarios. This suggests that, when confronted with the path-finding or more general planning task with a given goal, the Transformer learns the structural information to associate the next step with both the current step and the goal, enabling it to generate the subsequent task step. Nevertheless, the Transformer’s limitation in learning only the observed reachability matrix, without deducing the complete reachability matrix, hints at potential constraints on the goal-oriented information it can acquire. This limitation may result in the Transformer failing to grasp novel reachability relationships derived from the transitivity of reachability relations. In the next section, we will further verify the effectiveness of the Transformer in the path-finding task through extensive empirical evaluations.

## 5 Empirical Evaluations: Peeking into a Trained Transformer

We conduct extensive experiments on the path-finding task using the general Transformer architecture as described in Section 2.1. The experiments include tests on the overall accuracy of the Transformer model for the path-finding task, as well as investigation on how well the model learns the attention and the structural information about the adjacency and reachability matrices. In this section, we present these empirical evaluation results, which show that the results derived from our theoretical analysis in Section 4 can be carried over to the general Transformer architecture.

### 5.1 Datasets

#### 5.1.1 Graphs

The graph is generated randomly on two parameters: the number of nodes  $n$ , and the probability of edge  $p = 0.05$ . Given these two parameters, we generate a DAG with  $n$  nodes as follows: for any  $1 \leq i < j \leq n$ , there is an edge  $(i, j) \in \mathcal{E}$  with probability  $p$ , and the randomness for different edges are independent.

#### 5.1.2 Training Data and Test Data

Given the DAG, we first find all the possible reachable pairs  $(s, t)$  (i.e.,  $s \neq t$  and there exists at least one path that starts at  $s$  and ends at  $t$ ). Then these reachable pairs are separated into the training set (w.p. 0.5) and the test set (w.p. 0.5), but if edge  $(s, t) \in \mathcal{E}$ , we always put  $(s, t)$  in the training set. For a reachable pair  $(s, t)$  in the training set, we generate  $m = 20$  random paths that start at  $s$  and end at  $t$ , and put these  $m$  paths into the training dataset. When generating the random path, at each current node  $i$ , we find all the possible  $k \in \mathcal{V}$  such that  $\mathbf{A}_{(i,k)} = 1$  and  $\mathbf{R}_{(t,k)} = 1$  (i.e., there is an edge  $(i, k) \in \mathcal{E}$ , and  $k$  could also reach the target  $t$ ), and uniformly choose a random one from them. Moreover, we always put the one-edge path “ $s \ t \ s \ t \ \backslash n$ ” in the training dataset for each  $(s, t) \in \mathcal{E}$ , to guarantee that all edges appear at least once in the training data.

### 5.2 Accuracy on Test Dataset

We train Transformer models on the the aforementioned training dataset and subsequently evaluate performance of these models using the pairs in the test dataset. For test pair  $(s, t)$ , The correctness of a models’ output is determined based on its validity in terms of syntax and whether it corresponds to a valid path from  $s$  to  $t$ . In our experiments, we employ Transformer models with an embedding size of  $d = 120$ . We conduct tests using various configurations, ranging from 1-layer and 1-head to 6-layer and 6-head, while considering different graph sizes, with number of nodes  $n$  ranging from 100 to 500. The accuracy results on all these tests are presented in Figure 3. From these results, we make the following observation:

- When comparing the five figures, we note that the accuracy tends to decrease as the number of nodes increases. For  $n = 100$  and  $200$ , the accuracy consistently remains above 0.95. However for  $n = 300$ , the accuracy drops to a range between 0.91 and 0.95, and for  $n = 400$  and  $500$ , the accuracy further declines to a range between 0.80 and 0.90 in most cases.
- When examining at each row, we observe that the accuracy remains relatively stable even as the number of attention heads increases.
- Upon examining each column, we observe that when the embedding size is sufficiently large in comparison to the graph size (e.g.,  $n = 100, 200$ ), the accuracy remains relatively stable as the number of layers increases. Conversely, when the embedding size is small comparing to the graph size (e.g.,  $n = 300, 400, 500$ ), the accuracy shows a slight improvement as the number of layers increases. Specifically, the accuracy with  $L = 3, 4, 5, 6$  layers tends to be slightly higher than the accuracy achieved with  $L = 1$  and  $2$  layers.

The above observations suggest that both the embedding size and the number of layers have an impact on the model’s accuracy, as they influence the number of parameters in the model. On the one hand, when the embedding size is sufficiently large compared to the graph size, even 1-layer 1-head

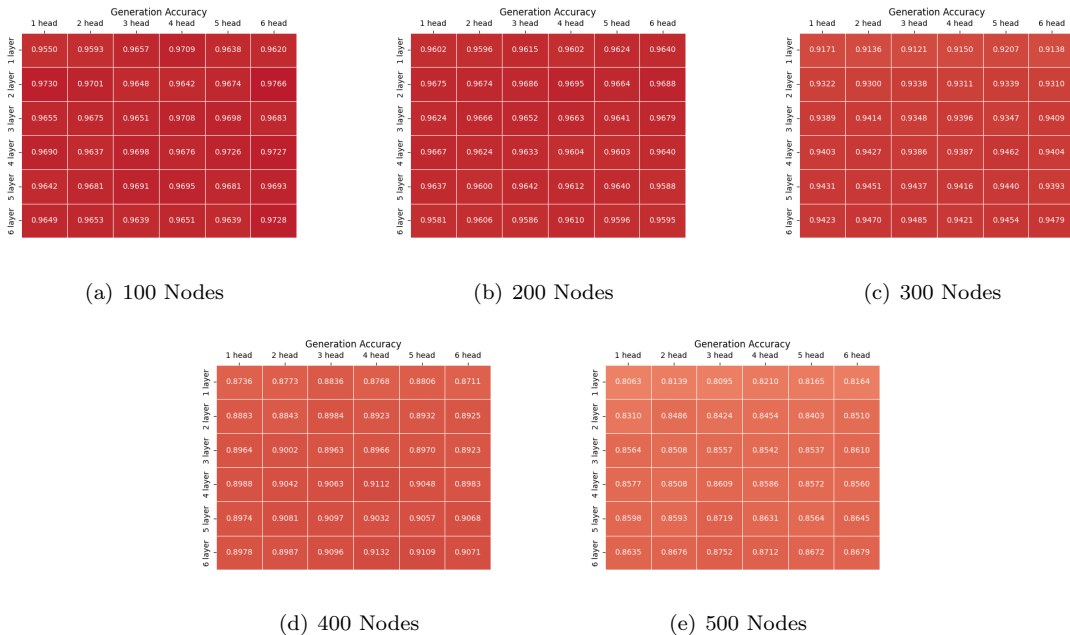


Figure 3: Accuracy on the test dataset with embedding size  $d = 120$ . **Takeaway:** when the embedding size is large enough, even a Transformer with 1 layer and 1 head can achieve good accuracy; when the embedding size is not large enough, even a Transformer with 6 layers and 6 heads is not enough to achieve good accuracy.

models would perform well. This coincides with our theoretical analysis in the previous section, which shows that when the embedding size equals to the graph size, the 1-layer and 1-head structure is enough to predict the next nodes accurately. On the other hand, our empirical results show that when the embedding size is small comparing to the graph size, the Transformer architecture may need more parameters to increase the accuracy, which could be achieved by increasing the number of layers in the model. However, increasing the number of layers does not efficiently increase the accuracy a lot, e.g., the accuracy for Transformer with 3 layers is almost the same as the accuracy for Transformer with 6 layers.

### 5.3 Attention

We now look inside the Transformer models, and try to find more evidence that our theoretical analysis reflects the reality. In our theoretical analysis, we assume that the attention is fixed on the target node. Is it true for the Transformer models learned from read data? The corresponding results are shown in Figure 4. These results are obtained by looking into the attention mechanism of the five 1-layer and 1-head Transformer models, and showing the average (taking on the test dataset) matrix of  $\text{softmax}\left(\frac{QK^T}{\sqrt{d_k}}\right)$ , of which the  $n^{\text{th}}$  row represents the attention vector for predicting the  $(n + 1)^{\text{th}}$  token.

Note that the second column in these figures represents the attention weights on the second token, which corresponding to the target node in our test data. We can see that, when predicting the next tokens, almost all the attention weights are concentrated on this column, especially for those models with higher accuracy (Figure 4(a) for  $n = 100$  and Figure 4(b) for  $n = 200$ ). This demonstrates that indeed the Transformer model learns the correct attention for the path-finding task, and our assumption on the attention for the theoretical analysis is reasonable.

### 5.4 Adjacency Matrix

Our analysis in Section 4 shows that the observed adjacency matrix and the observed reachability matrix are stored in the feed-forward layer and the attention layer. We now verify this on the general

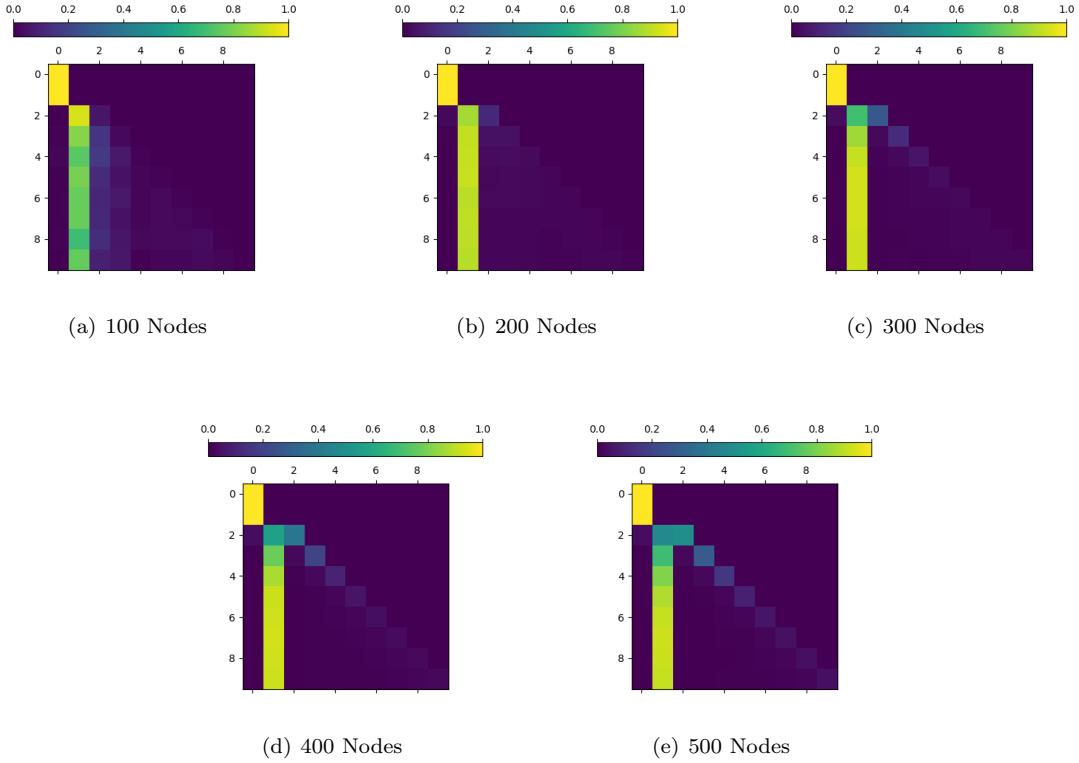


Figure 4: The average attention in 1-layer and 1-head Transformer. **Takeaway:** the Transformer could let its attention concentrate on the target node, especially when the embedding size is large enough.

1-layer and 1-head Transformer model that includes all the Transformer mechanisms, such as attention weights, non-linear transformation, token and position embedding.

Note that in the Transformer layer, the output can be written as <sup>4</sup>

$$\text{FFN} \left( \text{softmax} \left( \frac{QK^\top}{\sqrt{d_k}} \right) V + X \right) + \text{softmax} \left( \frac{QK^\top}{\sqrt{d_k}} \right) V + X.$$

Also noting that we have verified that the attention is concentrated at the second token, then we let  $X_2 = U_{(2,:)} W_t$ , representing the token embedding of the target node, and  $X_n = U_{(n,:)} W_t$ , representing the token embedding of the current node. Then we know that

$$\hat{u}_{(n+1)} \approx (\text{FFN}(X_2 W^V + X_n) + X_2 W^V + X_n) W_o.$$

It is straightforward that  $X_n W_o$  contains the information of current node, and  $X_2 W^V W_o$  contains the information of the target node. As for  $\text{FFN}(X_2 W^V + X_n) W_o$ , we choose to use its linear approximation as  $\text{FFN}(X_2 W^V + X_n) W_o \approx \text{FFN}(X_2 W^V) W_o + \text{FFN}(X_n) W_o$ . As shown by Table 1 (which takes average over all possible  $X_2$ 's and  $X_n$ 's), this is a good approximation. Then we can treat  $\text{FFN}(X_2 W^V) W_o$  as the information of the target node, and  $\text{FFN}(X_n) W_o$  as the information of the current node.

Table 1: Average Cosine Similarity of  $\text{FFN}(X_2 W^V + X_n)$  and  $\text{FFN}(X_2 W^V) + \text{FFN}(X_n)$

Graph	100 Nodes	200 Nodes	300 Nodes	400 Nodes	500 Nodes
<b>Average Cosine Similarity</b>	0.926	0.924	0.901	0.870	0.889

<sup>4</sup>For simplicity, though the layer normalizations  $LN_1, LN_2$  and  $LN_t$  are used in our experiments, we omit them in the equations.

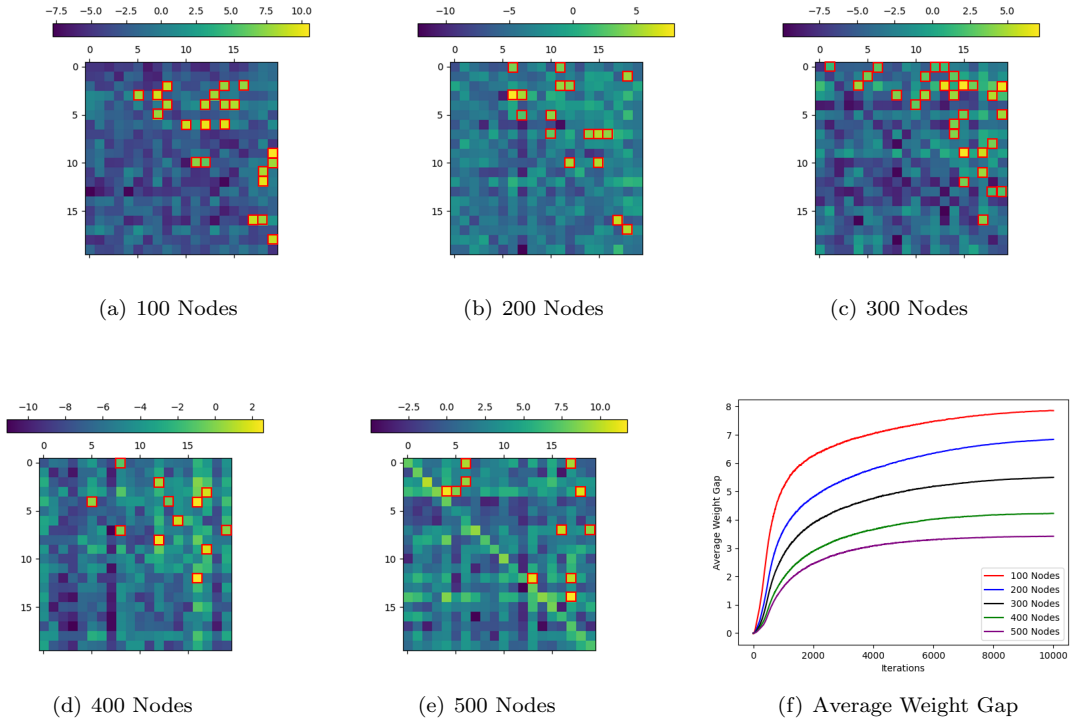


Figure 5: The first 20 rows and columns of  $\mathbf{W}^{M'}$  matrix in 1-layer and 1-head Transformer (the red boxes correspond to 1's in the adjacency matrix  $\mathbf{A}$ ), and the average weight gap between edge terms and non-edge terms in  $\mathbf{W}^{M'}$ . Takeaway: the adjacency matrix is stored in the FFN layer.

In this subsection, we want to verify that the adjacency matrix is stored in the feed-forward layer, i.e., in the sum of two terms  $\text{FFN}(\mathbf{X}_n) \mathbf{W}_o + \mathbf{X}_n \mathbf{W}_o$ . Let  $\mathbf{W}^{M'}$  be the matrix whose  $i$ -th row is  $\text{FFN}(\mathbf{e}_i^\top \mathbf{W}_t) \mathbf{W}_o + (\mathbf{e}_i^\top \mathbf{W}_t) \mathbf{W}_o$ , where  $\mathbf{e}_i$  represents the one-hot column vector for node  $i$  (with dimension  $M = |\mathcal{V}| + 1$ ). Note that in the simplified Transformer model of Section 4,  $\mathbf{W}^{M'}$  is the same as matrix  $\mathbf{W}^M$ . The results of  $\mathbf{W}^{M'}$  are shown in Figure 5.

As we can see, in Figure 5(a), the  $\mathbf{W}^{M'}$  matrix and the adjacency matrix are highly aligned: almost all the large entries in the  $\mathbf{W}^{M'}$  matrix correspond to real edges, and almost all real edges correspond to large entries in the  $\mathbf{W}^{M'}$  matrix. This high accuracy is because the embedding size  $d = 120$  is higher than the number of nodes  $n = 100$ . If the embedding size is lower than the graph size (Figures 5(b), 5(c), 5(d) and 5(e)), we inevitably lose some accuracy when approximating the adjacency matrix by the product of matrices with rank smaller than the graph size, let alone the non-linear layers' influence. Even so, there is still high relevance between  $\mathbf{W}^{M'}$  and the adjacency matrix: most real edges correspond to large entries in the  $\mathbf{W}^{M'}$  matrix.

In Figure 5(f), we show the gap between the average weight corresponds to edges (i.e., the average of  $\mathbf{W}_{(i,j)}^{M'}$ 's with  $i < j$  and  $(i, j) \in \mathcal{E}$ ) and the average weight corresponds to non-edges (i.e., the average of  $\mathbf{W}_{(i,j)}^{M'}$ 's with  $i < j$  and  $(i, j) \notin \mathcal{E}$ ). We can see that in all these five graphs, their gaps keep increasing until convergence, suggesting that weights between edges and non-edges are more easily separated as the learning process proceeds. Moreover, with lower number of nodes, the gap is higher. We believe this is because that when the embedding size is fixed, one can approximate the adjacency matrix better for smaller graphs.

## 5.5 Reachability Matrix

In this subsection, we want to verify that the reachability matrix is stored in the attention layer, i.e., in the two terms  $\mathbf{X}_2 \mathbf{W}^V \mathbf{W}_o + \text{FFN}(\mathbf{X}_2 \mathbf{W}^V) \mathbf{W}_o$ . Let  $\mathbf{W}^{V'}$  be the matrix whose  $i^{\text{th}}$  row is  $(\mathbf{e}_i^\top \mathbf{W}_i) \mathbf{W}^V \mathbf{W}_o + \text{FFN}((\mathbf{e}_i^\top \mathbf{W}_i) \mathbf{W}^V) \mathbf{W}_o$ , where  $\mathbf{e}_i$  represents the one-hot column vector for node  $i$



(with dimension  $M = |\mathcal{V}| + 1$ ). Note that in the simplified Transformer model of Section 4,  $\mathbf{W}^{V'}$  is the same as matrix  $\mathbf{W}^V$ .

In Figure 6(a), we show the average weights of three different sets in the graphs: “obs” corresponds to the  $\mathbf{W}_{(t,k)}^{V'}$ ’s with  $t \geq k$  and  $\mathbf{R}_{(t,k)}^{\text{obs}} = 1$ ; “real\obs” corresponds to the  $\mathbf{W}_{(t,k)}^{V'}$ ’s with  $t \geq k$ ,  $\mathbf{R}_{(t,k)}^{\text{obs}} = 0$  but  $\mathbf{R}_{(t,k)}^{\text{real}} = 1$ ; and “non” corresponds to the  $\mathbf{W}_{(t,k)}^{V'}$ ’s with  $t \geq k$  and  $\mathbf{R}_{(t,k)}^{\text{real}} = 0$ . Here we only show the results of graphs with 100 nodes and 200 nodes, since i) their accuracy is high enough (about 0.96, and does not become higher even if there are more layers/heads, as shown in Figures 3(a) and 3(b)); ii) their attention is quite close to be concentrate on the target node (see Figures 4(a) and 4(b)). When there are more nodes, the ability of approximating the reachability matrix is not enough for us to distinguish it. From these average weights, we can see that the Transformer learns  $\mathbf{R}^{\text{obs}}$  quite well, as for those terms in “real\obs”, their weights are almost the same as those in “non”. This echos our analysis in Section 4.

To further demonstrate that  $\mathbf{R}^{\text{real}}$  is not learned as good as  $\mathbf{R}^{\text{obs}}$ , we divide the source-target node pair  $(s, t)$  in the test dataset into four categories:

- Degree 0:  $\mathbf{R}_{(t,s)}^{\text{obs}} = 1$ .
- Degree 1:  $(s, t)$  is not of degree 0, while  $s$  has at least one out-neighbor node  $u$  such that  $(u, t)$  is of degree 0, i.e.  $\mathbf{R}_{(t,u)}^{\text{obs}} = 1$ .
- Degree 2:  $(s, t)$  is not of degree 0 and 1, while  $s$  has at least one out-neighbor node  $u$  such that  $(u, t)$  is of degree 1.
- Degree 3 or more: the remaining  $(s, t)$  pairs in the test dataset.

Roughly speaking, in our analysis, when the Transformer is predicting the next node of  $s$  for the source-target pair  $(s, t)$ , it will add the adjacency vector of  $s$  and the reachability vector of  $t$ , and use the sum as the weight vector of the next node. For  $(s, t)$  pairs of degree 0 or 1, we know that there is a node  $u$  such that  $(s, u) \in \mathcal{E}$  and  $\mathbf{R}_{(t,u)}^{\text{obs}} = 1$ . Then node  $u$  will have a large weight, indicating a high accuracy. On the other hand, for  $(s, t)$  pairs of degree 2 or more, there is no node  $u$  such that both its corresponding entry in the adjacency vector of  $s$  and its corresponding entry in the reachability vector of  $t$  are large. In this case, the high-weight entry when predicting the next node is either an adjacent node of  $s$  or a recorded node that can reach  $t$ . Since none of the recorded nodes reachable to  $t$  is adjacent to  $s$ , the accuracy for  $(s, t)$  pairs of degree 2 or more should be much lower than those of degree 0 or 1.

To see this, we check the accuracy of the Transformer on the  $(s, t)$  pairs of the four different categories. The results are shown in Figure 6 (b)-(f). In this figure, each row of the accuracy matrix is further divided into four sub-rows corresponding to the accuracy of degree-0 pairs, degree-1 pairs, degree-2 pairs, and degree-3 or more pairs respectively (in the graph with 100 nodes, there are no test  $(s, t)$  pairs in the degree-3 or more category). From these results, we can see that the accuracy for degree-2 pairs and degree-3 or more pairs is much lower than the two other categories in most cases. It indicates that, even with a larger model (e.g. 6-layer 6-head Transformer), the model has a fundamental difficulty to generate paths for high-degree source-target pairs, namely those pairs who can only be connected by concatenating several path segments in the training dataset. In short, the model fails to learn reachability through the transitivity among the reachability relations. This result demonstrates the validity of our theoretical analysis, which shows that the Transformer can only learn observed reachability, and will miss those unobserved reachability deduced from the transitivity of the reachability relation.

## 5.6 Summary of the Empirical Results

In summary, our extensive empirical evaluation leads to the following conclusions about the auto-regressive Transformer model in achieving the path-finding task: (a) With large enough embedding size, the model can achieve high accuracy in general; (b) The model achieves its performance by concentrating attentions on the target nodes as intended, and learning the information on adjacency and reachability matrices, just as what a human would do and as predicted by our theoretical analysis; and (c) The model may have limitations and fail to learn high-order reachability relations through transitivity, and thus fail to generate paths derived from high-order reachability, as human would expect.

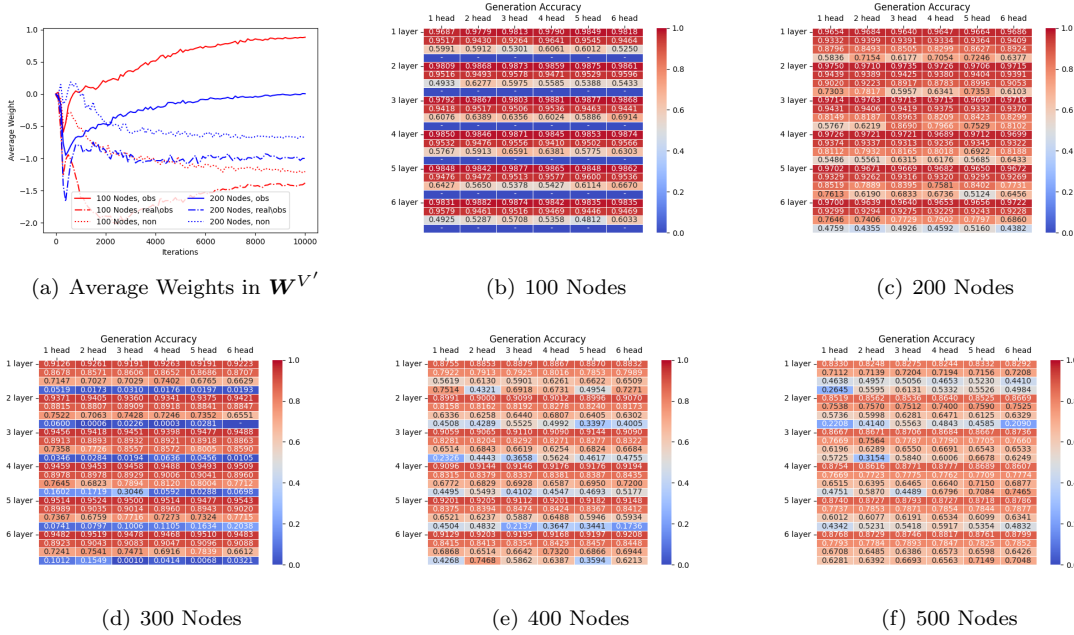


Figure 6: The average weights in  $\mathbf{W}^{V'}$ , and the accuracy for  $(s, t)$ 's with different degree. **Takeaway:** the Transformer can only store the observed reachabilities and cannot learn the non-observed reachabilities well.

## 6 Path-planning in Blocksworld

To further validate the theoretical results in Section 4 and the practicability of the proposed path-finding task, we consider Blocksworld benchmark [VMSK24]. Blocksworld is a scenario consisting of a set of blocks identified by different colors. The blocks are either placed on table or on top of another block and the task is to plan a block manipulation from the given state to the target state.

We formulate Blocksworld as a path-finding task. Here we construct a graph  $G_{BW}$  for the case with 4 blocks, where each node represents a state of the blocks. For example, node 0 refers to the state that “the red block is on top of the blue block, the blue block is on top of the orange block, the orange block is on top of the yellow block, and the yellow block is on the table”.  $G_{BW}$  is a directed graph with 73 nodes, and the adjacency matrix of  $G_{BW}$  is presented in Figure 7(a). Specifically, the states corresponding to the first 24 nodes are the states where the four blocks are stacked one on top of another in a single stack, and thus each of these nodes only has one out-neighbor corresponding to removing the top block and putting it on the table. The last node refers to the state where all blocks are on the table, so it has 12 out-neighbors, corresponding to the 12 states where three blocks are on the table and the fourth block is on top of one of the three blocks.

In the original Blocksworld task, the answer is a sequence of actions, which is equivalent to the notion of edges in  $G_{BW}$ . We reformulated it to let the model output a path from the given state to the target state, only consisting of the nodes. This can be seen as a simplified version and a pure planning task. We randomly select 80% of all node pairs for training and the rest 20% for testing and generate the 50000 training data in the same format as introduced in Section 5. We mainly use Transformers with 1 layer and 1 head for the convenience of visualization.

### 6.1 Results

We first present the accuracy during the training when using different embedding sizes  $d \in \{30, 60, 120\}$ . As is shown in Figure 7(d), although a smaller embedding size results in a longer time to converge, all models reach an accuracy near 100% at the end of the training.

Then, we use the same method introduced in Section 5 to visualize the attention map and the  $\mathbf{W}^{M'}$  matrix for the model with  $d = 120$  after the entire iterations. In Figure 7(c), we can see that when predicting the tokens on the path, almost all the attention weights are on the second token which

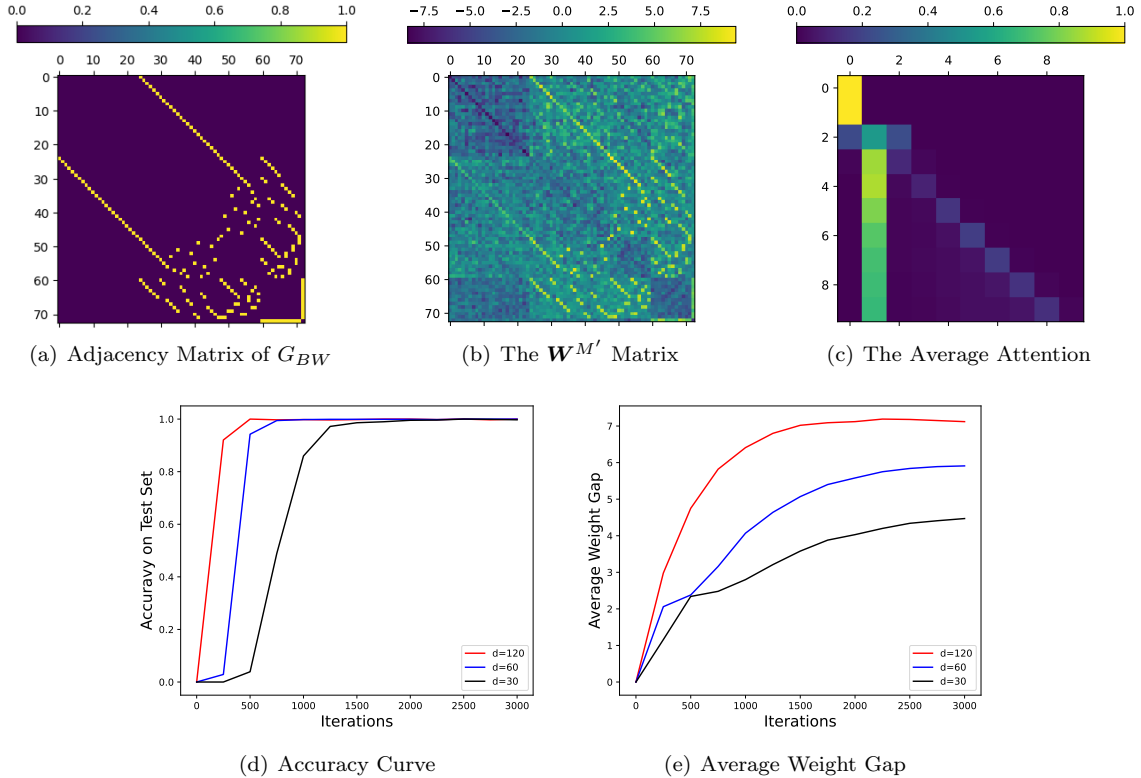


Figure 7: Accuracy, attention, and adjacency matrix results for the experiment on Blocksworld benchmark.

represents for the target node, demonstrating the capability of the model to learn a correct attention. For adjacency matrix, we find that the  $\mathbf{W}^{M'}$  matrix in Figure 7(b) almost perfectly aligns to the real adjacency matrix of  $G_{BW}$ . And the weight gap (average edge weight minus average non-edge weight) for all models keeps increasing in the training process until convergence, as is shown in Figure 7(e).

In addition, we present the results related to reachability matrix in Figure 8. Figure 8(a) shows the observed reachability in the training dataset. Although  $G_{BW}$  is fully-connected, some reachability are not observed since we request that all training data has no cycle. Specifically, each of the first 24 nodes is not observed reachable to any nodes other than itself. To validate whether Transformer has captured this information, we construct  $\mathbf{W}^{V'}$  matrix through the same method presented in Section 5. As shown in Figure 8(b), the  $\mathbf{W}^{V'}$  matrix has represented darkness for the first 24 columns, which aligns to the real observed reachability matrix. Furthermore, we plot the average gap between the weight of  $\mathbf{W}^{V'}$  on observed reachability and those exist but not observed in Figure 8(c). We find that this gap keeps increasing for all models<sup>5</sup>.

In summary, our experimental results on the Blocksworld benchmark confirms our theoretical analyses (Theorem 4) and empirical results on the synthetic data, and it at least partially explains the planning capability of the Transformer on the Blocksworld scenario.

## 7 Related Works

### 7.1 LLMs for Planning

Several recent studies have empirically evaluated the planning abilities of large language models (LLMs). For instance, CogEval has introduced a variety of planning tasks set in mazes and graphs, ultimately finding no evidence to suggest LLMs grasp the intricacies of the maps or the planning tasks

<sup>5</sup>Since there does not exist any test pairs that are with degree 2 or more (as defined in Section 5), we do not compare the accuracy between different degrees in Blocksworld.

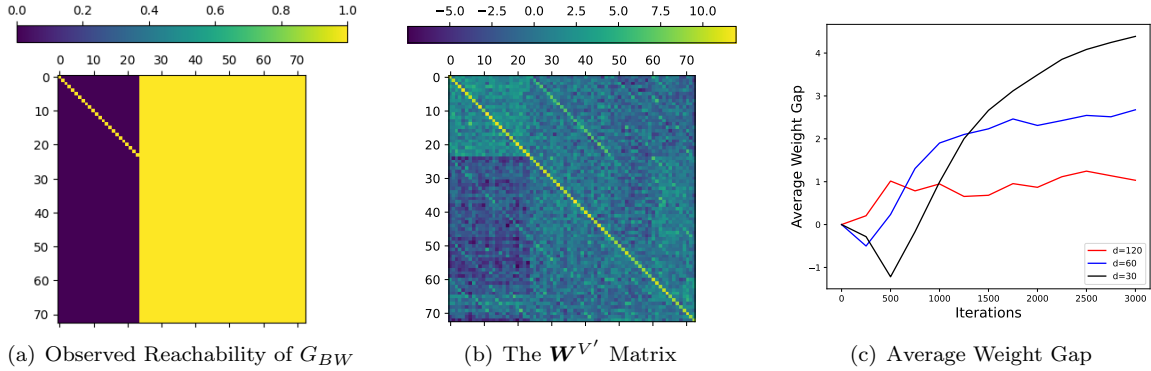


Figure 8: Reachability for the experiment on Blocksworld benchmark.

themselves [MHVF<sup>+</sup>23]. Similarly, another study explored the Blocksworld game, a planning challenge where humans typically achieve success rates above 70%, in stark contrast to GPT-3’s mere 5% success rate [VMSK24]. Our paper proposes a novel approach by formulating a class of planning problems as path finding on graphs, applying this model to the blocksworld game and uncovering significant insights, as detailed in Section 6.

Despite these seemingly negative evaluations, LLMs have shown remarkable aptitude in executing real-world planning tasks, creating the field of *autonomous agents* [WMF<sup>+</sup>24]. Certain applications of autonomous agents feature explicit graphs. In the tool agent HuggingGPT [SST<sup>+</sup>23], LLMs are deployed to trigger a sequence of external APIs in response to user requests. Here, APIs are conceptualized as graph nodes, with their interrelations represented as edges, and the selection process akin to identifying a path or subgraph that aligns with user demands. This scenario is an extension of the settings discussed in this paper, where the graph is text-attributed and the objective function is evaluated through textual analysis. The application of graph search techniques has been shown to enhance the performance of tool agents significantly [LLG<sup>+</sup>23, LPY<sup>+</sup>24]. The math agent Alpha-Geometry utilizes LLMs to solve geometry problems [TWL<sup>+</sup>24]. By treating lemmas as nodes and their interdependencies as edges, the process of finding a proof of a theorem is analogous to finding a path to the theorem node in the above graph formed by possible lemma nodes and their interdependency edges. However, [TWL<sup>+</sup>24] focuses on using LLM to generate auxiliary constructions, and the reasoning tasks are done by a non-LLM engine. This is very different to our research. There are no explicit graphs in other agents, such as game agents [WXJ<sup>+</sup>23], embodied agents [HAPM22], and code agents [SCG<sup>+</sup>24]. The core strategy in these domains is to employ verbal reinforcement learning within LLMs. It is noteworthy that any dynamic programming problem characterized by deterministic state transitions can be reformulated as a shortest path problem on a graph, with states and transitions represented as nodes and edges, respectively. As a result, the area of autonomous agents is closely related to the path-planning task investigated in this paper.

## 7.2 LLM for Graphs

GPT4Graph [GDL23] and NLGraph [WFH<sup>+</sup>23] have developed extensive frameworks for assessing LLMs in the context of graph tasks. These frameworks encompass a broad spectrum of challenges, including classic graph problems (e.g., connectivity, cycle detection, and topological sorting), graph neural network (GNN) tasks (e.g., node and graph classification), and semantic graph question answering (e.g., knowledge graph inquiries). They also explore various input formats, such as adjacency lists, edge lists, GML, and GraphML, alongside innovative prompting techniques like few-shot, role prompting, chain-of-thought, and algorithmic prompting (e.g., stating “we are using DFS”). These studies demonstrate that LLMs possess basic graph processing capabilities, and the choice of prompts and formats influence performance significantly. Yet, they also reveal the models’ susceptibility to spurious correlations within graphs. GPT-4, for instance, only achieves around 50% accuracy on shortest path tasks, even when utilizing complex prompts. To our knowledge, this paper presents the first theoretical analysis that identifies and explains the spurious correlations learned by LLMs (Theorem

3), supporting the negative outcomes reported in these studies.

There has also been a surge in efforts aiming at bolstering LLMs’ performance on graph tasks. Innovations like GraphGPT [TYW+23] and GraphLLM [CZW+23], which incorporate an additional GNN encoder, have shown notable improvements across the aforementioned graph tasks. GraphInstruct [LSH+24] seeks to enhance LLMs’ capabilities using pure LLM approaches. This involves meticulously documenting the steps of classical algorithms (e.g., BFS and DFS) and fine-tuning LLMs to learn these graph algorithms. This method of procedural supervision has extended the capacity of LLMs in graph tasks from the complexity class  $TC^0$  to P/poly [FZG+23]. However, while this approach has yielded performance improvements in simpler tasks such as topological sorting and connectivity, it has proven less effective for more complex challenges, like finding Hamiltonian Paths.

### 7.3 Algorithm Simulation with Transformers

Recent theoretical investigations have shed light on the capability of Transformer to simulate algorithms, a topic that has garnered considerable interest. This discussion begins with discrete algorithms. From a circuit complexity standpoint, Transformer models are likened to parallel circuits characterized by polynomial width and constant depth, which places them within the  $TC^0$  complexity class. It is also noticed that  $TC^0 \subseteq NC^1 \subseteq P$ . On the other hand, despite their impressive expressiveness, Transformer is theoretically incapable of addressing a range of P-complete problems, including the testing of Context-Free Grammar Membership [MS23]. However, the advent of chain-of-thought prompting has enabled Transformer to sequentially simulate algorithms, thereby equipping them to tackle P-complete problems in domains such as arithmetic and decision-making [FZG+23]. The exploration extends to continuous algorithms, where it has been demonstrated that Transformer can approximate functions such as matrix inversion, Stochastic Gradient Descent (SGD), and power iterations [GRS+23]. Our study specifically applies GPT models to simulate path-finding algorithms, presenting evidence that their expressiveness is sufficient for such tasks (Theorem 2). Nevertheless, the usage of auto-regressive loss and gradient descent introduces certain limitations (Theorem 3), which have not been studied in existing works.

### 7.4 Mechanisms of LLMs

LLMs have demonstrated capabilities that exceed the theoretically predicted lower bounds of expressiveness. To demystify this paradox, numerous studies have employed experimental methodologies akin to those used in the physical and biological sciences. Their aim is to decode the mechanisms of LLMs. The foundational strategy is to generate controlled synthetic datasets to analyze how language models (not necessarily the LLMs) complete various tasks. Standard methods for this analysis include visualizing attention patterns to examine computational properties (such as locality and time invariance) and employing linear probing on the hidden states to determine the extent of learning. Given that the data is synthetic and the ground-truth mappings are generally known, it becomes feasible to isolate the influence of various factors (e.g., prompting strategies, chain-of-thought reasoning, and data formatting). For example, a dataset designed for learning group operations, as detailed in [ZBB+22], facilitates the exploration of how pretraining, data composition, and neural architecture influence reasoning tasks within LLMs. Similarly, the generation of synthetic context-free grammar (CFG) data, as described in [AZL23a], enables training GPT-2 models, uncovering their capacity to learn dynamic programming algorithms for parsing CFGs. Synthetic datasets focusing on biographical knowledge, presented in [AZL23b, AZL23c, AZL24], probe into the mechanisms of knowledge storage, retrieval, manipulation, and the implications of scaling laws. Moreover, the work in [LSL+23] introduces synthetic datasets aimed at understanding how smaller LLMs tackle basic arithmetic operations, like addition, and examines the effects of few-shot prompting, pretraining, and model scaling [LSL+23]. This paper builds upon these investigations by conducting controlled experiments with a path planning dataset, thereby shedding light on the complexities and challenges of planning in LLMs.

## 8 Discussion and Conclusion

In this paper, we present our investigation on how the Transformer architecture executes the path-finding task, which abstracts a number of planning tasks one may encounter in practical scenarios.

We first show that the Transformer has the expressive power of path finding by manually construct a 1-layer 1-head Transformer that encodes the adjacency matrix and the reachability matrix with its weight matrices. Next we provide a theoretical analysis demonstrating that the Transformer can indeed learn the adjacency matrix and the observed reachability matrix (a limited form of reachability) from the path training data through the common gradient descent mechanism on cross-entropy loss function. We then verify our theoretical analysis through comprehensive experiments, both on synthetical network data and on a concrete Blocksworld planning benchmark. Our empirical findings support our theoretical analysis and demonstrate that the Transformer can achieve high accuracy in many cases, it can concentrate its attention correctly to the target node, and it extracts adjacency matrix and observed reachability matrix as predicted by our theoretical analysis. Our theoretical analysis further points out a limitation of the Transformer — it cannot learn well the transitive reachability, and this point is validated by our experimental results.

Our study is the first to combine theoretical analysis with empirical evaluation on such planning tasks. In particular, we are the first to apply theoretical analysis using the gradient descent learning method of the Transformer on a concrete task and provide theoretical interpretation, which is validated by our experimental results. More importantly, our theoretical analysis is able to unveil a potential limitation of the Transformer in completing the path-finding task, which guides us to verify that indeed this limitation occurs in the experiments. This demonstrates the power of theoretical analysis as a guidance for understanding practical Transformers and LLMs.

Although the path-finding task is a simple task on a network and our investigation is still the first attempt to understand Transformer’s capability on this task, our findings may already provide some insights and implications to path finding and planning in general. We can see that, due to the autoregressive nature of learning, the Transformer cannot execute path finding by a simple trial-and-error search such as depth-first or breadth-first search, and thus it has to plan ahead well in generating the next node on the path correctly. We demonstrate that the Transformer can adjust its effort accordingly by concentrating its attention to the target, and generating the next node that is both adjacent to the current node and reachable to the target, mimicking the human intelligence. It suggests that for many planning tasks in general, the Transformer architecture is adjusting its learning by balancing the consideration between the immediate continuation of the next step and its final goal of reaching the target.

Our investigation opens up many possible future directions, and we list several of them below. (a) Extend our study to hyper-graphs and hyper-paths, where a hyper-edge models the situation in which several preconditions need to be satisfied together in order to carry out the next step, which is common in task planning and mathematical proofs. (b) Further understand the limitation of the Transformer on path finding: the current inability of transitive reachability may be due to the limited expressive power of the path language, and it may also suggest the fundamental difference between Transformer’s interpretation and human’s interpretation on path finding. This requires further study, perhaps by enriching the languages, or by an investigation on the deployed LLMs such as GPT4. It can also stimulates new improvement to the Transformer architecture to achieve better performance. (c) Study the connection between the abstract path-finding task and some concrete planning tasks (e.g. block moving in Blocksworld, etc.), to see if Transformer has any capability of abstracting a concrete task to the more abstract path-finding task, or find if what Transformer does for concrete planning tasks has any commonalities with the abstract path-planning task. (d) Study deployed LLMs or fine-tune LLMs to connect their planning capabilities with our path-finding investigation.

We are planning to deepen our investigation on the above fronts. We also hope that our work could inspire more people to study LLMs with combined theoretical and empirical analysis, with the ultimate goal of understanding and explaining the power of LLMs.

## References

- [AZL23a] Zeyuan Allen-Zhu and Yuanzhi Li. Physics of language models: Part 1, context-free grammar. *arXiv preprint arXiv:2305.13673*, 2023.
- [AZL23b] Zeyuan Allen-Zhu and Yuanzhi Li. Physics of language models: Part 3.1, knowledge storage and extraction. *arXiv preprint arXiv:2309.14316*, 2023.

- [AZL23c] Zeyuan Allen-Zhu and Yuanzhi Li. Physics of language models: Part 3.2, knowledge manipulation. *arXiv preprint arXiv:2309.14402*, 2023.
- [AZL24] Zeyuan Allen-Zhu and Yuanzhi Li. Physics of language models: Part 3.3, knowledge capacity scaling laws. *arXiv preprint arXiv:2404.05405*, 2024.
- [BCE<sup>+</sup>23] Sébastien Bubeck, Varun Chandrasekaran, Ronen Eldan, Johannes Gehrke, Eric Horvitz, Ece Kamar, Peter Lee, Yin Tat Lee, Yuanzhi Li, Scott Lundberg, Harsha Nori, Hamid Palangi, Marco Tulio Ribeiro, and Yi Zhang. Sparks of artificial general intelligence: Early experiments with GPT-4. *arXiv preprint arXiv:2303.12712*, 2023.
- [CZW<sup>+</sup>23] Ziwei Chai, Tianjie Zhang, Liang Wu, Kaiqiao Han, Xiaohai Hu, Xuanwen Huang, and Yang Yang. GraphLLM: Boosting graph reasoning ability of large language model. *arXiv preprint arXiv:2310.05845*, 2023.
- [FZG<sup>+</sup>23] Guhao Feng, Bohang Zhang, Yuntian Gu, Haotian Ye, Di He, and Liwei Wang. Towards revealing the mystery behind chain of thought: a theoretical perspective. *Advances in Neural Information Processing Systems*, 36, 2023.
- [GDL23] Jiayan Guo, Lun Du, and Hengyu Liu. Gpt4graph: Can large language models understand graph structured data? an empirical evaluation and benchmarking. *arXiv preprint arXiv:2305.15066*, 2023.
- [GRS<sup>+</sup>23] Angeliki Giannou, Shashank Rajput, Jy-yong Sohn, Kangwook Lee, Jason D Lee, and Dimitris Papailiopoulos. Looped transformers as programmable computers. In *International Conference on Machine Learning*, pages 11398–11442. PMLR, 2023.
- [HAPM22] Wenlong Huang, Pieter Abbeel, Deepak Pathak, and Igor Mordatch. Language models as zero-shot planners: Extracting actionable knowledge for embodied agents. In *International Conference on Machine Learning*, pages 9118–9147. PMLR, 2022.
- [LLG<sup>+</sup>23] Zhaoyang Liu, Zeqiang Lai, Zhangwei Gao, Erfei Cui, Zhiheng Li, Xizhou Zhu, Lewei Lu, Qifeng Chen, Yu Qiao, Jifeng Dai, et al. ControlLLM: Augment language models with tools by searching on graphs. *arXiv preprint arXiv:2310.17796*, 2023.
- [LPY<sup>+</sup>24] Xukun Liu, Zhiyuan Peng, Xiaoyuan Yi, Xing Xie, Lirong Xiang, Yuchen Liu, and Dongkuan Xu. ToolNet: Connecting large language models with massive tools via tool graph. *arXiv preprint arXiv:2403.00839*, 2024.
- [LSH<sup>+</sup>24] Zihan Luo, Xiran Song, Hong Huang, Jianxun Lian, Chenhao Zhang, Jinqi Jiang, Xing Xie, and Hai Jin. Graphinstruct: Empowering large language models with graph understanding and reasoning capability. *arXiv preprint arXiv:2403.04483*, 2024.
- [LSL<sup>+</sup>23] Nayoung Lee, Kartik Sreenivasan, Jason D Lee, Kangwook Lee, and Dimitris Papailiopoulos. Teaching arithmetic to small transformers. *arXiv preprint arXiv:2307.03381*, 2023.
- [MHVF<sup>+</sup>23] Ida Momennejad, Hosein Hasanbeig, Felipe Vieira Frujeri, Hiteshi Sharma, Nebojsa Jojic, Hamid Palangi, Robert Ness, and Jonathan Larson. Evaluating cognitive maps and planning in large language models with CogEval. *Advances in Neural Information Processing Systems*, 36, 2023.
- [MS23] William Merrill and Ashish Sabharwal. The parallelism tradeoff: Limitations of log-precision transformers. *Transactions of the Association for Computational Linguistics*, 11:531–545, 2023.
- [SCG<sup>+</sup>24] Noah Shinn, Federico Cassano, Ashwin Gopinath, Karthik Narasimhan, and Shunyu Yao. Reflexion: Language agents with verbal reinforcement learning. *Advances in Neural Information Processing Systems*, 36, 2024.
- [SST<sup>+</sup>23] Yongliang Shen, Kaitao Song, Xu Tan, Dongsheng Li, Weiming Lu, and Yueting Zhuang. HuggingGPT: Solving AI tasks with ChatGPT and its friends in Huggingface. *Advances in Neural Information Processing Systems*, 36, 2023.

- [TWL<sup>+</sup>24] Trieu H Trinh, Yuhuai Wu, Quoc V Le, He He, and Thang Luong. Solving Olympiad geometry without human demonstrations. *Nature*, 625(7995):476–482, 2024.
- [TYW<sup>+</sup>23] Jiabin Tang, Yuhao Yang, Wei Wei, Lei Shi, Lixin Su, Suqi Cheng, Dawei Yin, and Chao Huang. GraphGPT: Graph instruction tuning for large language models. *arXiv preprint arXiv:2310.13023*, 2023.
- [VMSK24] Karthik Valmeekam, Matthew Marquez, Sarath Sreedharan, and Subbarao Kambhampati. On the planning abilities of large language models-a critical investigation. *Advances in Neural Information Processing Systems*, 36, 2024.
- [WFH<sup>+</sup>23] Heng Wang, Shangbin Feng, Tianxing He, Zhaoxuan Tan, Xiaochuang Han, and Yulia Tsvetkov. Can language models solve graph problems in natural language? *Advances in Neural Information Processing Systems*, 36, 2023.
- [WMF<sup>+</sup>24] Lei Wang, Chen Ma, Xueyang Feng, Zeyu Zhang, Hao Yang, Jingsen Zhang, Zhiyuan Chen, Jiakai Tang, Xu Chen, Yankai Lin, et al. A survey on large language model based autonomous agents. *Frontiers of Computer Science*, 18(6):1–26, 2024.
- [WXJ<sup>+</sup>23] Guanzhi Wang, Yuqi Xie, Yunfan Jiang, Ajay Mandlekar, Chaowei Xiao, Yuke Zhu, Linxi Fan, and Anima Anandkumar. Voyager: An open-ended embodied agent with large language models. *arXiv preprint arXiv:2305.16291*, 2023.
- [ZBB<sup>+</sup>22] Yi Zhang, Arturs Backurs, Sébastien Bubeck, Ronen Eldan, Suriya Gunasekar, and Tal Wagner. Unveiling Transformers with LEGO: a synthetic reasoning task. *arXiv preprint arXiv:2206.04301*, 2022.